

Simulation of the modern climate. Comparison with observations and data of other climate models

Volodin E.M.

1. Simulation of the modern climate using the Coupled General Circulation Model INM-CM3.0

Let us consider the simulation of the climate of XIX-XX centuries, or more exactly for the time period from 1871 until 2000, using a numerical model. At first we would like to look at the last 50 years of the simulation, i.e. the years from 1951 to 2000. The comparison is produced for the same period employing the NCEP reanalysis data. The climate is characterized by a large number of parameters, and it seems to be hard to consider all of them in the framework of one paper. So we would like to regard here only the most important, in our opinion, climate parameters. First of all we consider the state of the atmosphere, then the state of the ocean and finally some phenomena in the atmosphere-ocean system.

The Fig. 1.1 shows the sea level pressure for December-February obtained from observations and from the model, as well as the difference between them. We can see that the model reproduces well the main centers of action, such as the Iceland and Aleutian cyclones, Siberian and Canadian anticyclones, subtropical anticyclones of the southern hemisphere and subarctic low pressure cell. The model error more than 5 mb occurs only in separate places, and in the tropics it is in general not increasing 2 mb. In the temperate zone the largest errors are located in Eurasia and Atlantic, where the pressure is underestimated by 5-8 mb, and also in the Antarctic coastal zone, where it can be grow up to 5-8 mb. As a whole, the pressure simulation error of the coupled model is close to the corresponding error of the atmospheric model with the fixed SST.

The mean annual error of simulation of the zonal mean temperature in the troposphere (Fig. 1.2) does not exceed 2 degrees with the exception of the Arctic and Antarctic, where the temperature is underestimated by 2-4 degrees. The same underestimation of temperature exists over the southern subtropics and in the tropics of the upper troposphere. It should be noted that the underestimation of temperature by 5-10 degrees at the high latitudes close to the tropopause, which is clearly visible in the figure, takes place for all models, but the reason of this error is not clear so far. The zonal wind speed error in the troposphere does not exceed 2 m/s with the exception of the Southern Hemisphere, where the west wind velocity at the middle latitudes is underestimated by 2-4 m/s. Errors become much larger in the stratosphere. The west wind velocity in the middle latitudes of the Southern Hemisphere as well as the east wind velocity in the tropics are overestimated by 5-10 m/s. Such errors of zonal temperature and wind speed simulation are close to the error average over all models represented in the IPCC Fourth Assessment Report. Here, as in the previous case, the simulation error of the coupled model is close to the corresponding error of the atmospheric model with the fixed SST or slightly greater in magnitude.

It is important that the model must be able to reproduce not only average geophysical parameters, but also their variability. Observation and model standard deviations of the monthly sea-level pressure in December-February are presented in Fig. 1.3 The maximum variability is observed in the middle and high latitudes of the Northern Hemisphere and reaches 8 mb. The model standard deviation of pressure in the Northern Hemisphere is close to the observations. A small error of the model consists in the more northern location of the variability peaks. The model underestimates the

pressure variability in the Southern Hemisphere by 20-25%. It can be explained because in contrast to winter hemisphere, the variability in the summer hemisphere is caused by small eddies which can not be reproduced by the low-resolution model. Additional experiments show that this error disappears when the model has resolution of 2.5x2 degrees in latitude and longitude. The variability of pressure in the middle and high latitudes of the winter hemisphere is 10-15% less for the coupled model in comparison with the similar atmospheric model with the fixed SST and sea ice distribution. This is caused by the weak negative feedback between anomalies of the atmospheric circulation and SST in the middle latitudes. A small decrease of annual variability in the coupled model in comparison with the atmospheric model with the fixed SST takes place also in the other models.

The structure of the long-period variability is defined by the leading EOFs. The first two EOFs of the monthly sea-level pressure in the middle latitudes of the Northern Hemisphere in December-March obtained from observations and model are shown in Fig. 1.4 The first EOF has the negative anomaly of pressure at high latitudes and the positive one in the subtropics. It has maxima over Atlantic and Pacific Ocean (Arctic Oscillation or AO). The structure of the model first EOF is close to the observed, but the maximum in the subtropics of the Pacific Ocean is stronger in the model. Variance explained by the first EOFs constructed from the model and observation data are very similar (25 and 23%). Regarding the atmospheric model with the fixed SST we can see that the first EOF also represents AO, but the corresponding explained variance amounts to 34% this means that the negative feedback exists between the atmosphere and the ocean at the deviation of the index of AO.

The second EOF has a maximal amplitude at the north of the Pacific Ocean. It explains much less variance than the first one. According to the model data the maximum of the amplitude of the second EOF is also located at the north of the Pacific Ocean. The second EOF of the geopotential in the upper troposphere represents the Pacific - North American teleconnection pattern (PNA).

Anomalies of zonal wind speed in the Northern Hemisphere in the winter period, which are associated with the index of AO, take place not only near the surface, but also in the whole troposphere and stratosphere. The observational and model first EOFs of the zonal wind speed and the winter temperature are shown in Fig. 1.5. The first EOF of the zonal wind speed represents the positive anomaly of the wind speed at the middle latitudes from the surface up to the level of 10 mb, and the negative anomaly in the subtropics. The first EOF of temperature has the maximum in the lower polar stratosphere. The model data are close to observations both in the representation of the spatial distribution and in the explained variance corresponding to the first EOF.

We would like to note that for the atmospheric model with the fixed SST the explained variance, corresponding to the first EOFs of the zonal wind speed and temperature, is more on 10-20% than in the coupled model.

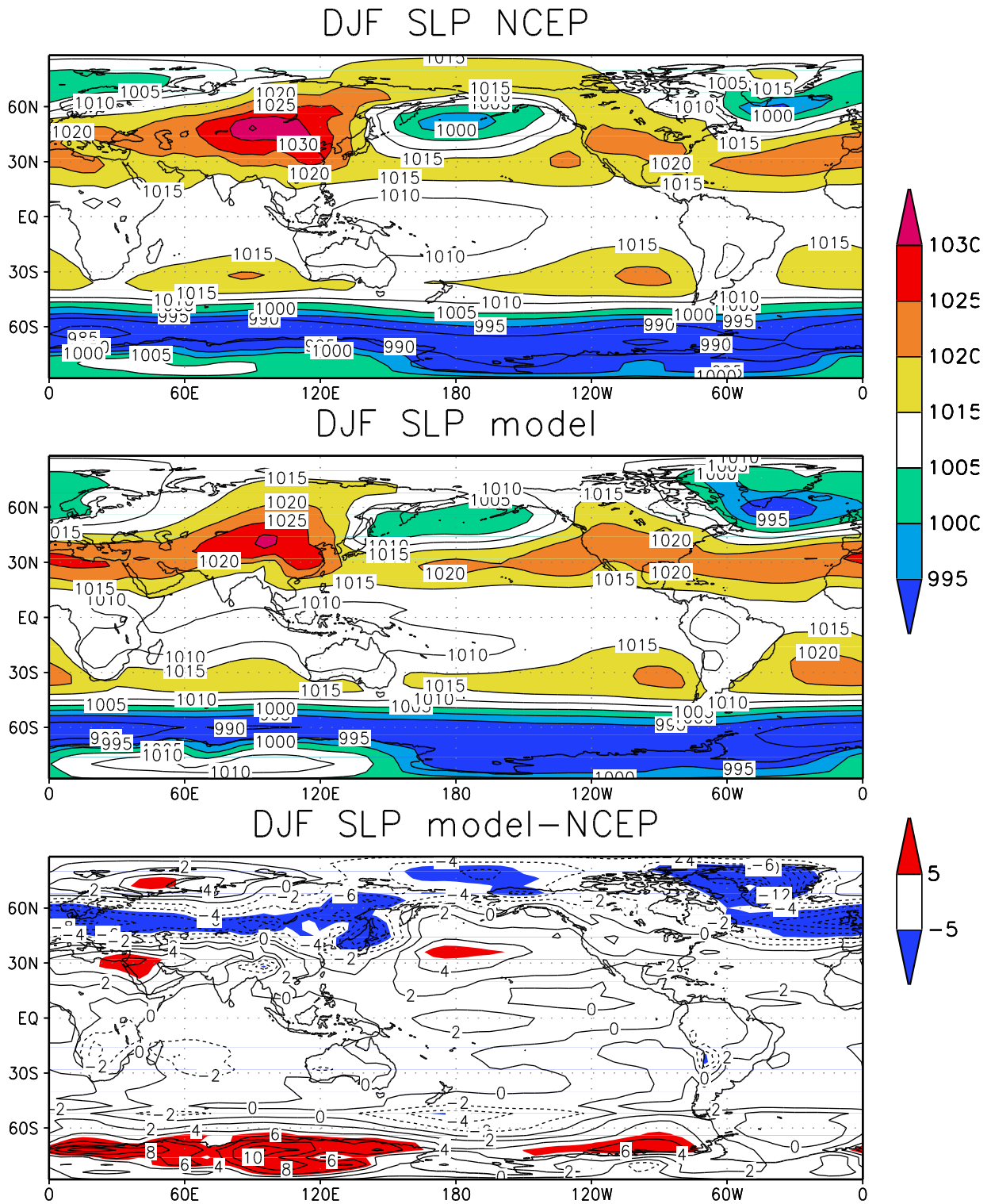


Fig. 1.1 Sea level pressure (mb) in December-February. The upper plot corresponds to the reanalysis data, the middle one — to the model and lower one shows the difference between them.

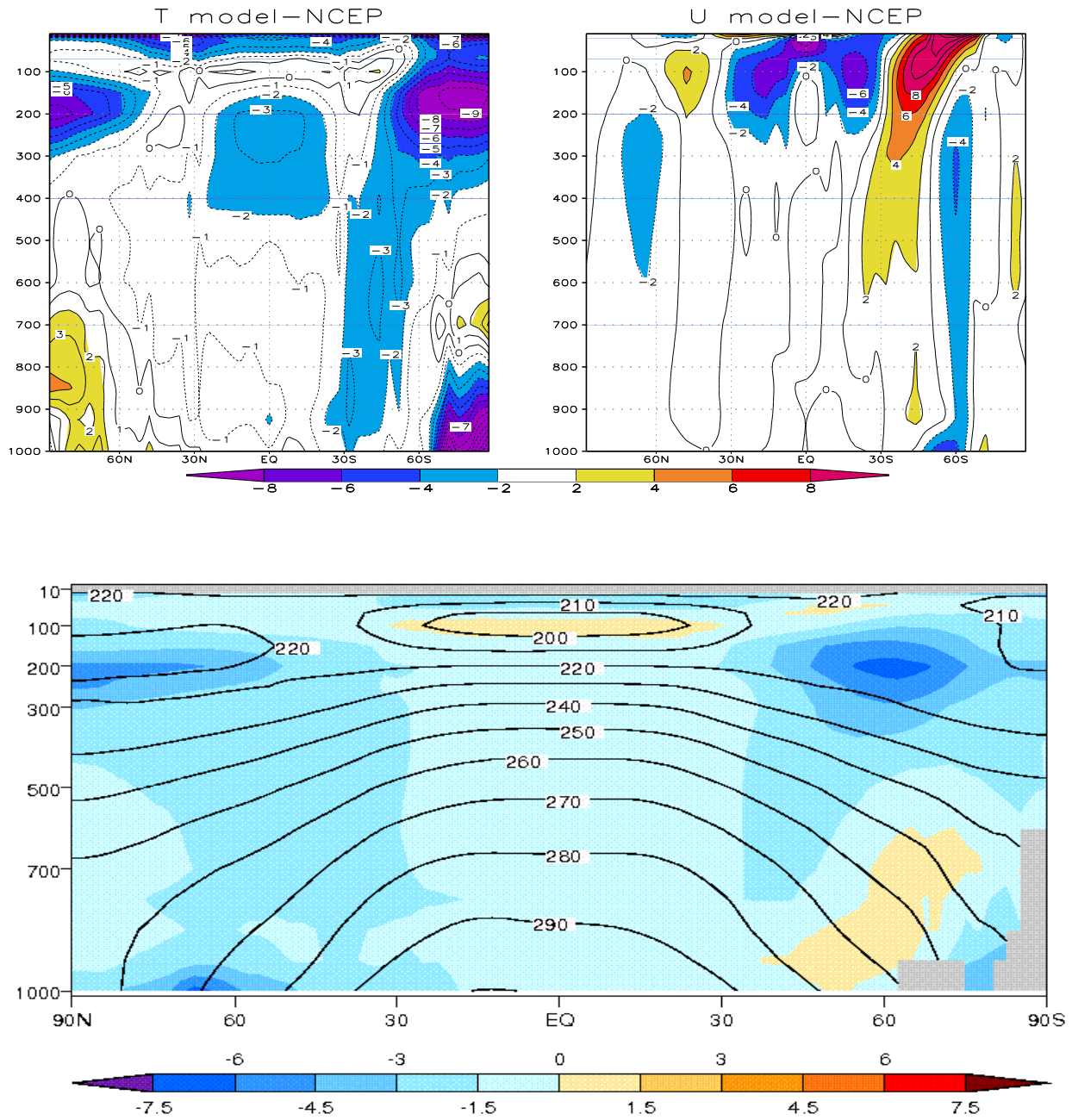


Fig. 1.2 The upper is mean annual anomalies of the zonal average temperature (left) and zonal wind speed (right) obtained from the model and reanalysis data. The lower is mean error of temperature obtained from all models.

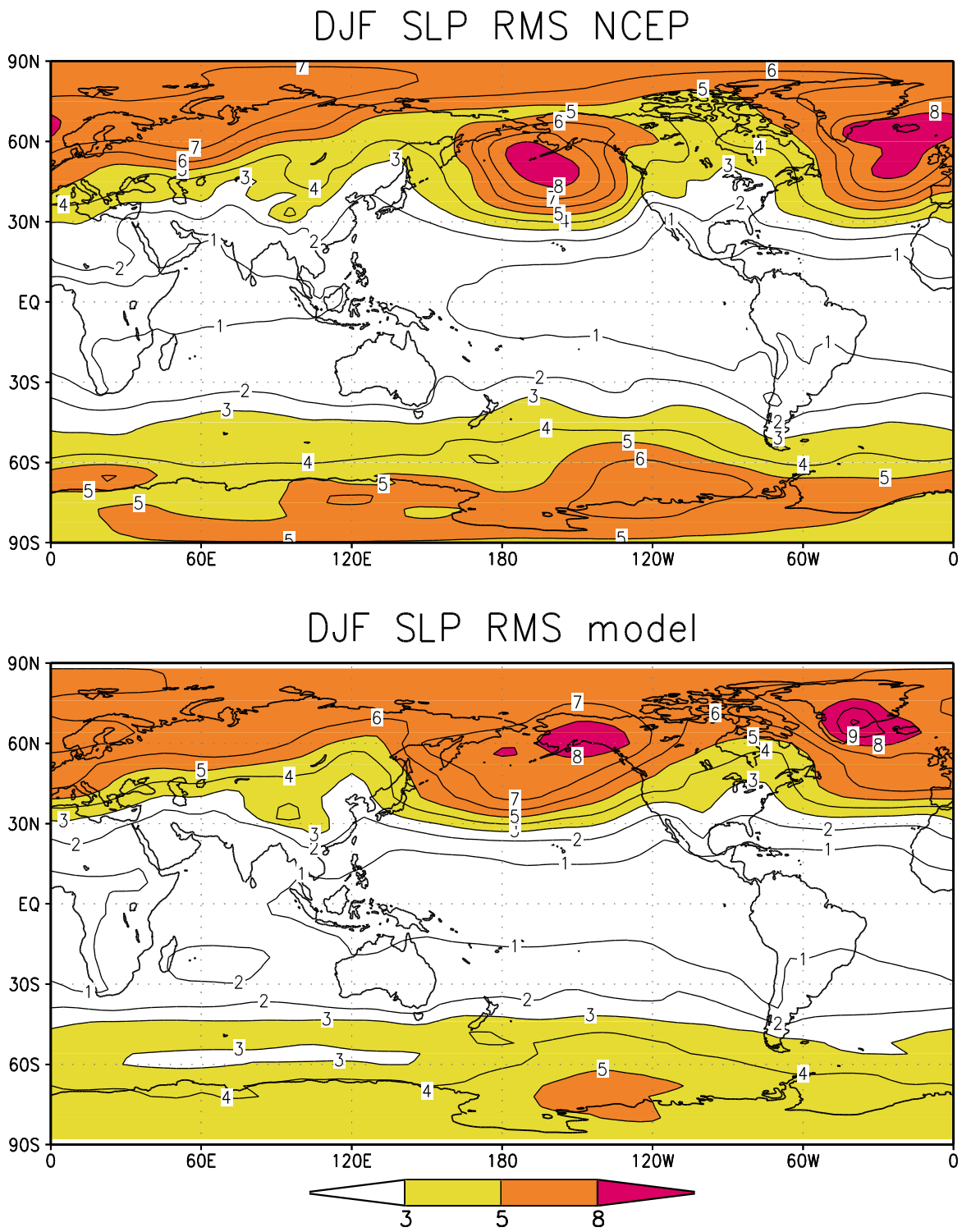


Fig. 1.3 Standard deviation of the monthly mean sea level pressure (mb) in December-February obtained from the NCEP reanalysis (upper) and the model data (lower).

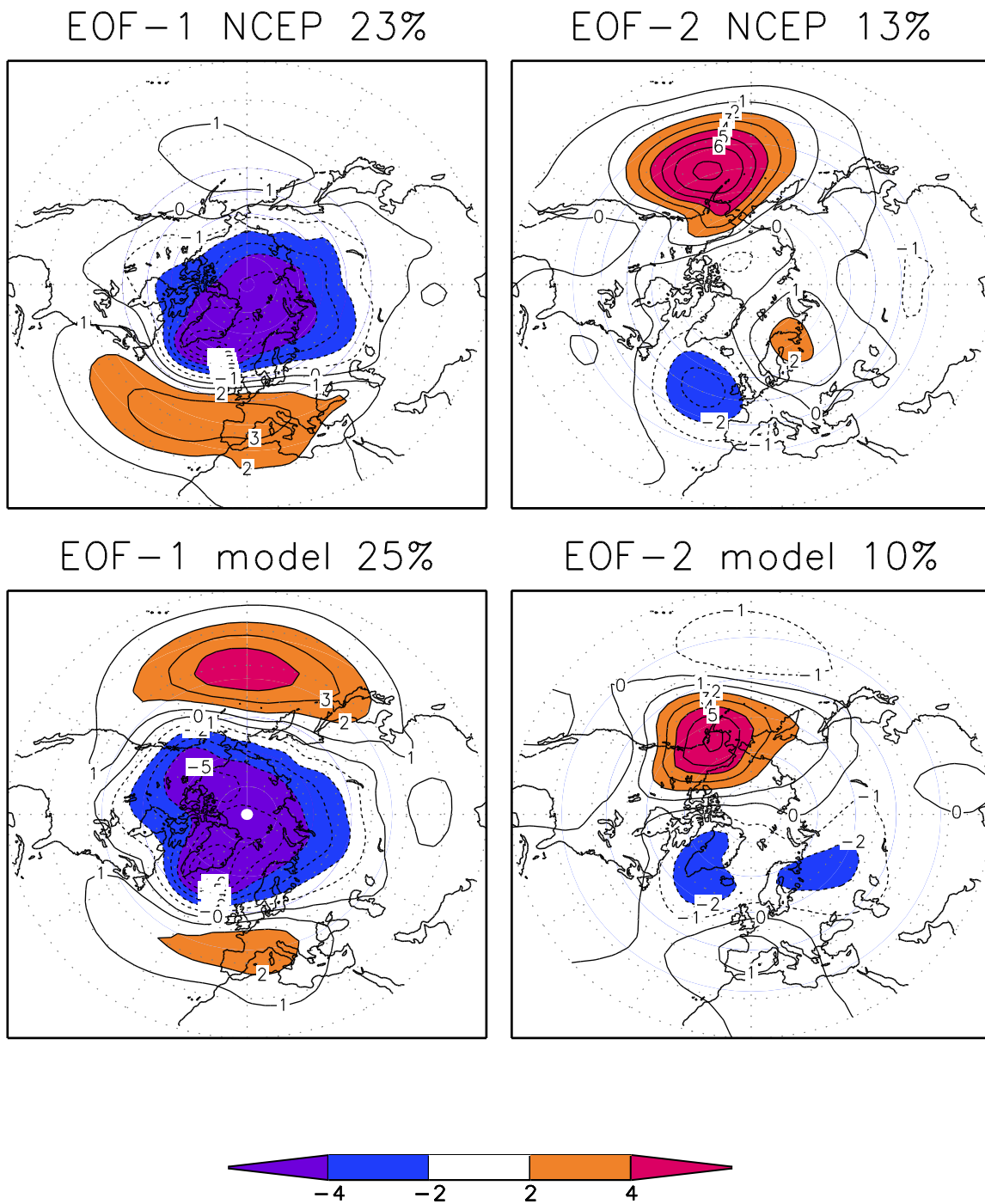


Fig. 1.4 The first (right) and the second (left) EOFs of the monthly mean sea level pressure in December-March obtained from observations (upper) and model data (lower).

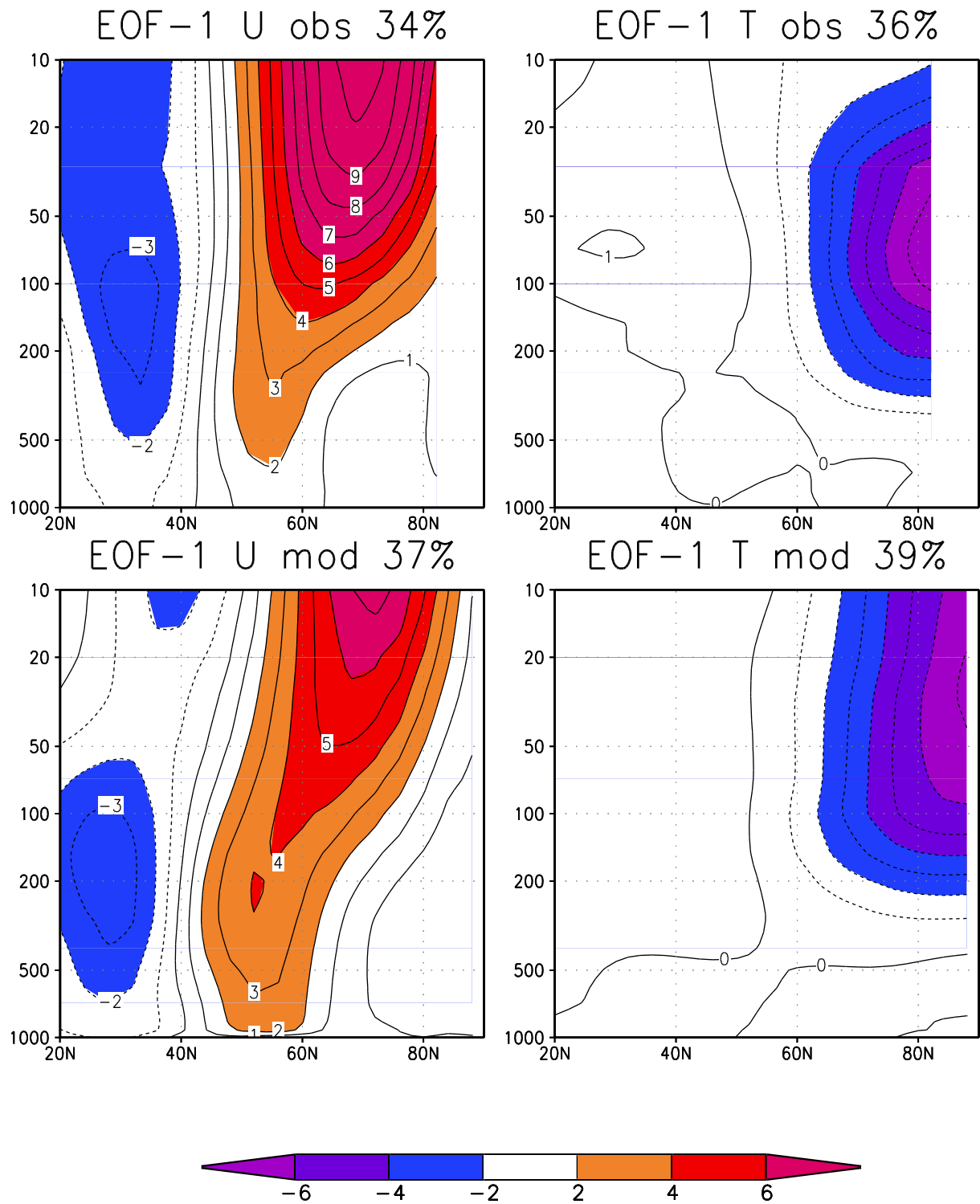


Fig. 1.5 The leading EOFs of the zonal wind speed (left) and temperature (right) in the December-March obtained from observations (upper) and model data (lower).

The Coupled General Circulation Model is first of all characterized by error of simulation of SST (Fig. 1.6). This error does not exceed 2 degrees in most regions, with the exception of Northwest Atlantic, where the overestimation is about 4-6 degrees. It is related with artificial correction of the fresh water in the Greenland and Norwegian seas. Furthermore, the temperature at the middle latitudes of the Southern Ocean and in the tropics at the east coast of the Pacific Ocean is overestimated by 2-4 degrees and it is underestimated by 2 degrees in the subequatorial zone of the Pacific Ocean. Such errors are common for the most modern models. The underestimation of temperature in the Pacific Ocean occurs because of the low resolution of the ocean model, which should be more than 0.5 degrees, for the adequate simulation of the subequatorial circulation and upwelling. Overestimation of temperature in the Southern Ocean and in the east of the Pacific Ocean is caused by inadequate description of the surface cloudiness under conditions of the temperature inversion.

Arctic sea ice distribution in the model is not far from the observed one. The shortcoming of the model is the more intensive melting of the ice at the end of summer which can be explained by overestimation of summer temperature in the north of Eurasia and America by 2-4 degrees. Also we can see that the Barents Sea freezing in winter is stronger than the observed one, but at the same time there is no ice at the east coast of Greenland that can be connected with absence of dynamics of the ice and inadequate simulation of the currents in the west Arctic.

Simulation of the sea ice in Antarctic (Fig. 1.8) agrees well with the observed one, because the influence of the ice dynamics and ocean on the ice behavior is not so important as in Arctic.

The zonal error of simulation of the temperature and salinity in the ocean is shown in Fig. 1.9. The water near the surface, especially in the tropics and subtropics, is more cold and fresh by the model data than by observations. The model water at large depths is warmer and more salted, especially at the middle latitudes. The exception is some regions at the middle latitudes of Northern Hemisphere where the water is warmer and more salted in all depths. Temperature errors are in general 1-2 degrees, the salinity errors amount to 0.5-1.0 ppm.

The barotropic stream function is shown in Fig. 1.10. The total model transport of the circumpolar current is around 80 Sv that is less than the estimate by observations (135 Sv), it is probably caused by overestimation of the bottom friction. The model transport of the Gulf Stream amounts to 50 Sv and it is about 60 Sv for the Kuroshio Current.

The interaction of the ocean and the atmosphere in the North Atlantic is described by leading SVD modes of the sea level pressure and SST (Fig. 1.11). The first mode of pressure represents the North Atlantic Oscillation (NAO) both by the model data and by observations. The positive phase of NAO corresponds to the negative anomaly of SST near the Canada and Africa, and also the positive anomaly of SST to the east of USA and to the west of Europe. In summary it can be concluded that the model data agree well with observations.

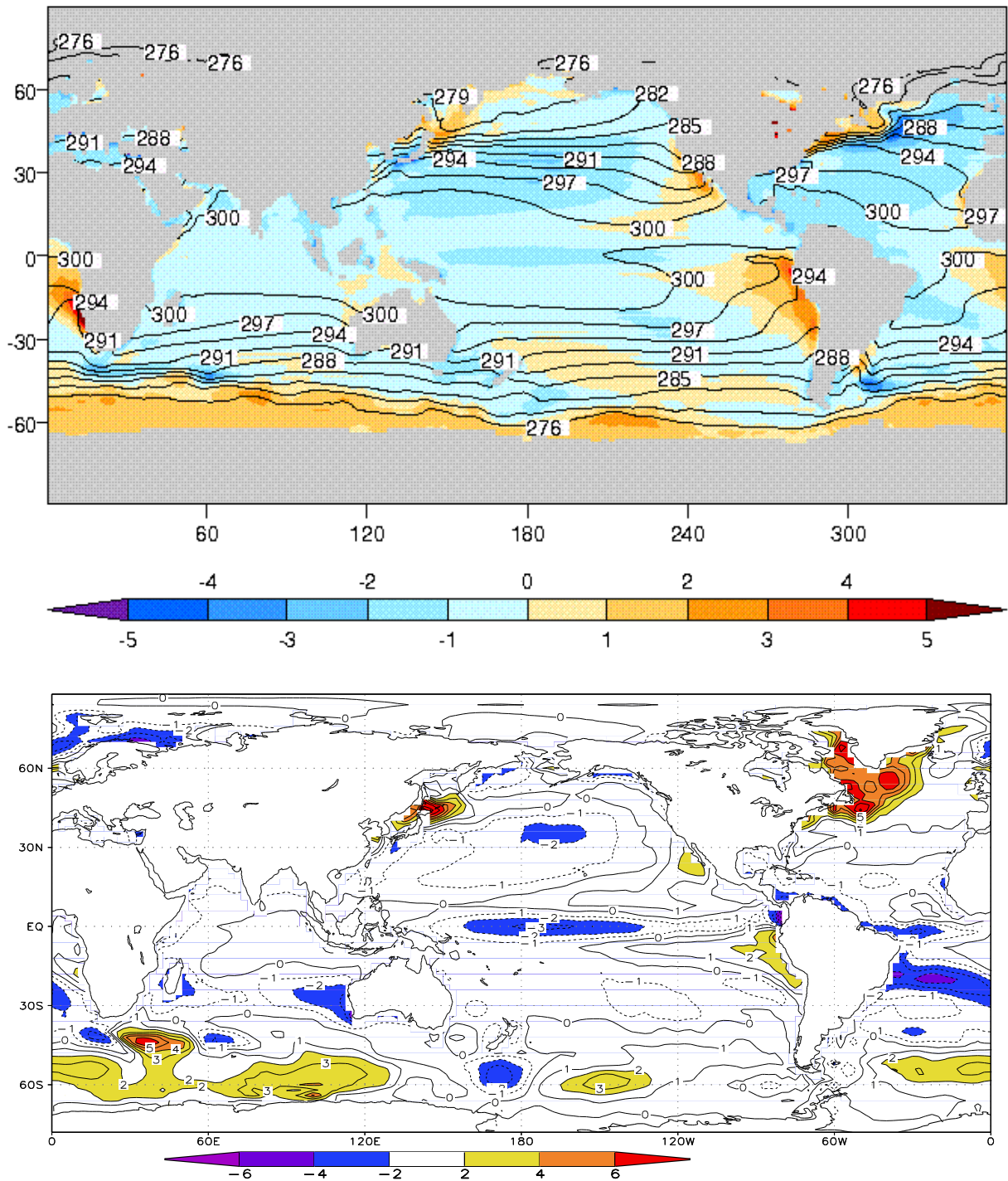


Fig. 1.6 The mean annual error of simulation of SST (K) for INM-CM3.0 (lower) and the mean error for all models(upper).

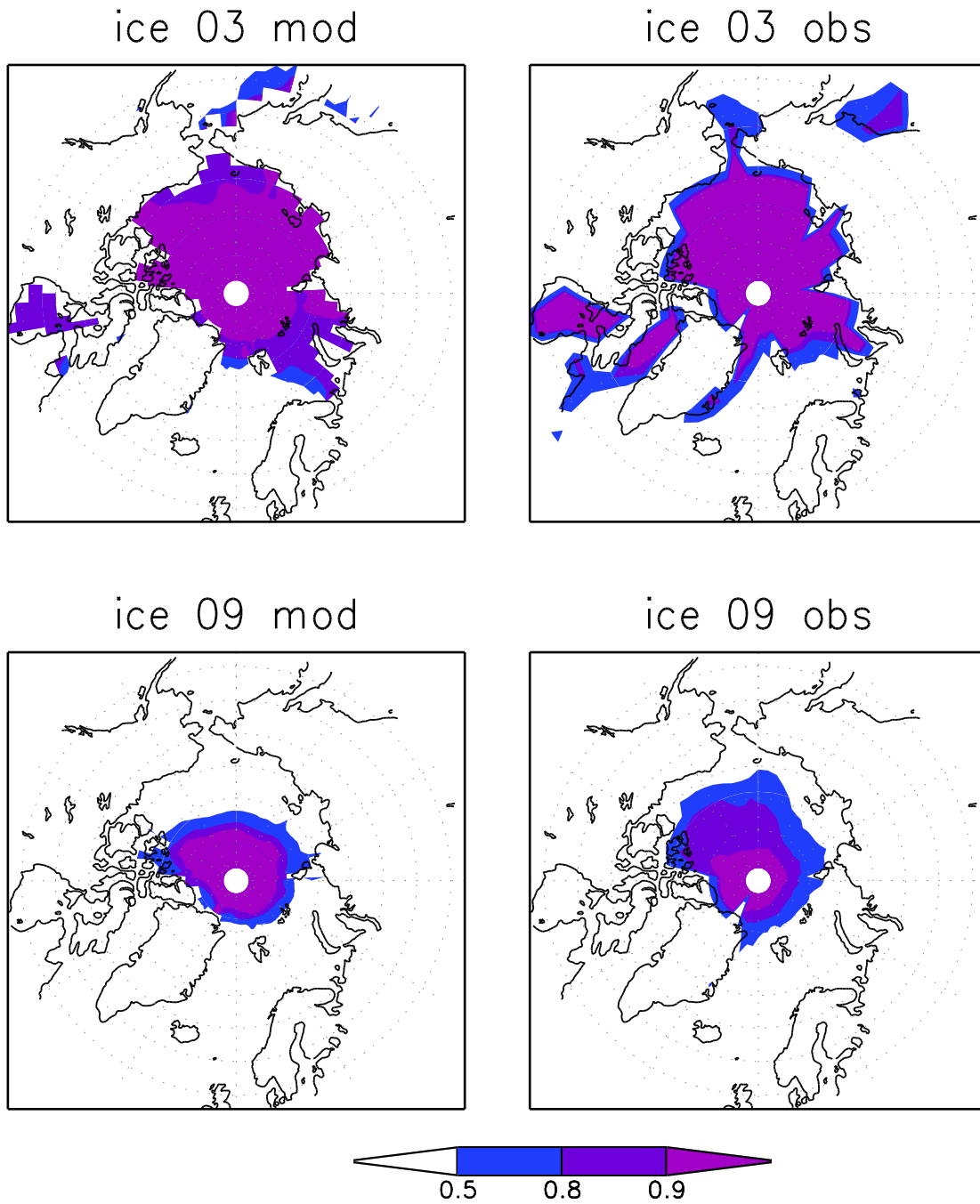


Fig. 1.7 The mean concentration of the sea ice in the Arctic in March (upper) and September (lower) obtained from the model data (left) and observations (right).

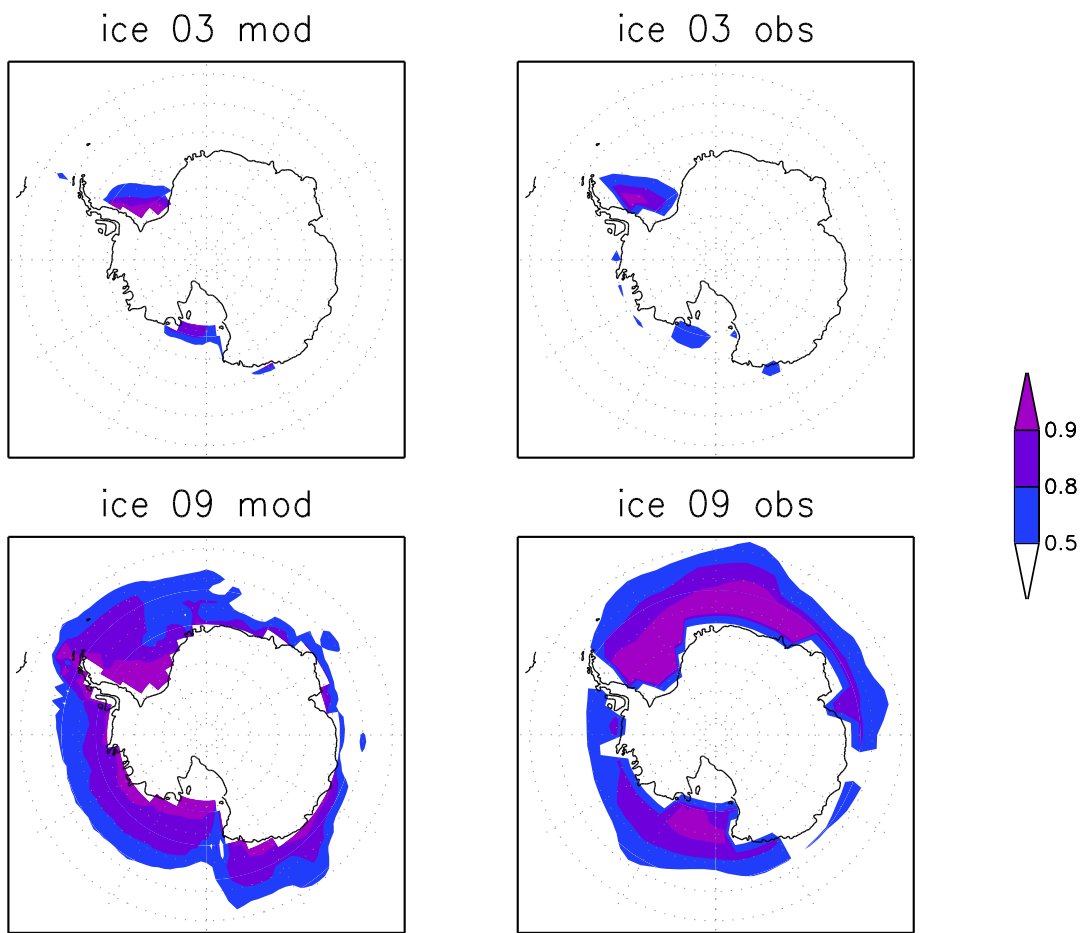


Fig. 1.8 The same as in Fig.7, but in Antarctic.

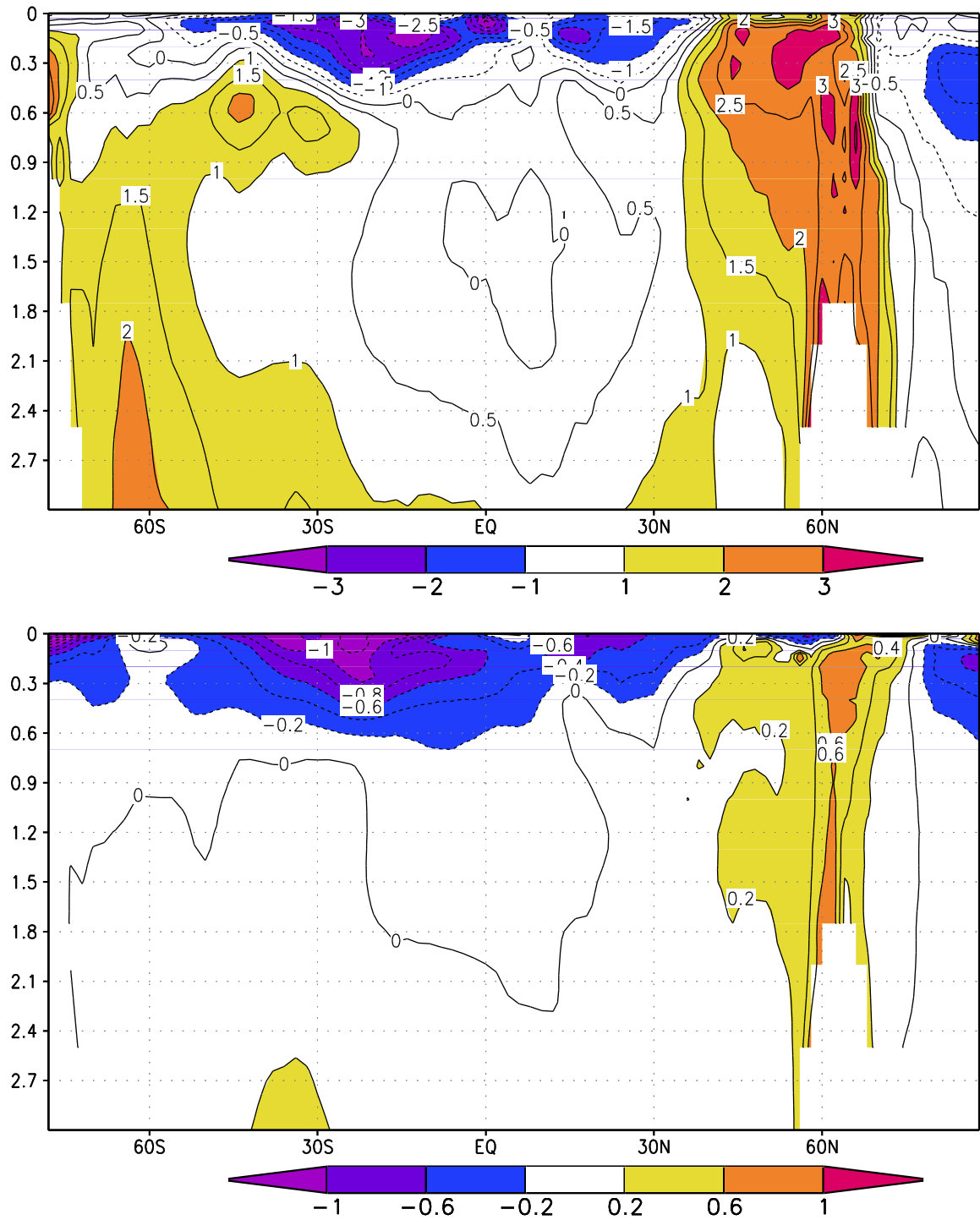


Fig. 1.9 Mean annual zonal error of temperature (upper, K) and salinity (lower, ppm) in the ocean.

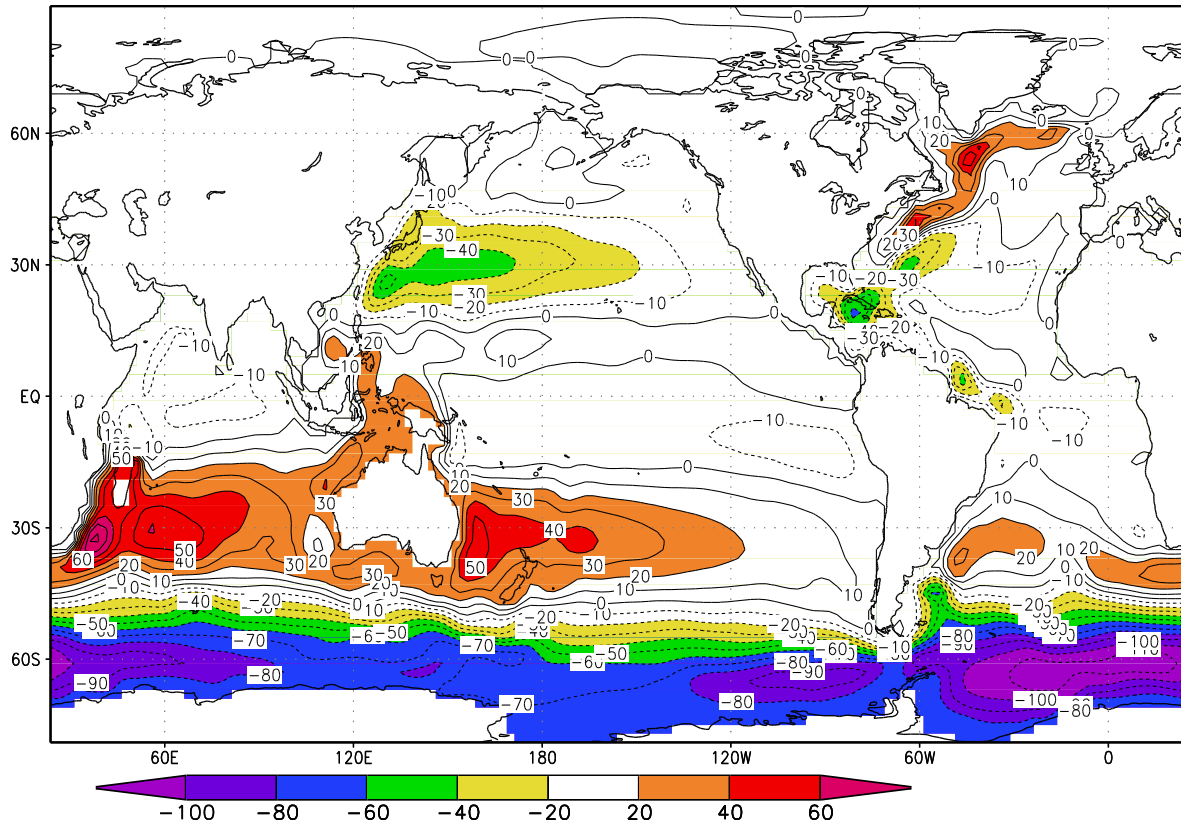


Fig. 1.10 Barotropic stream function (Sv) in the ocean model.

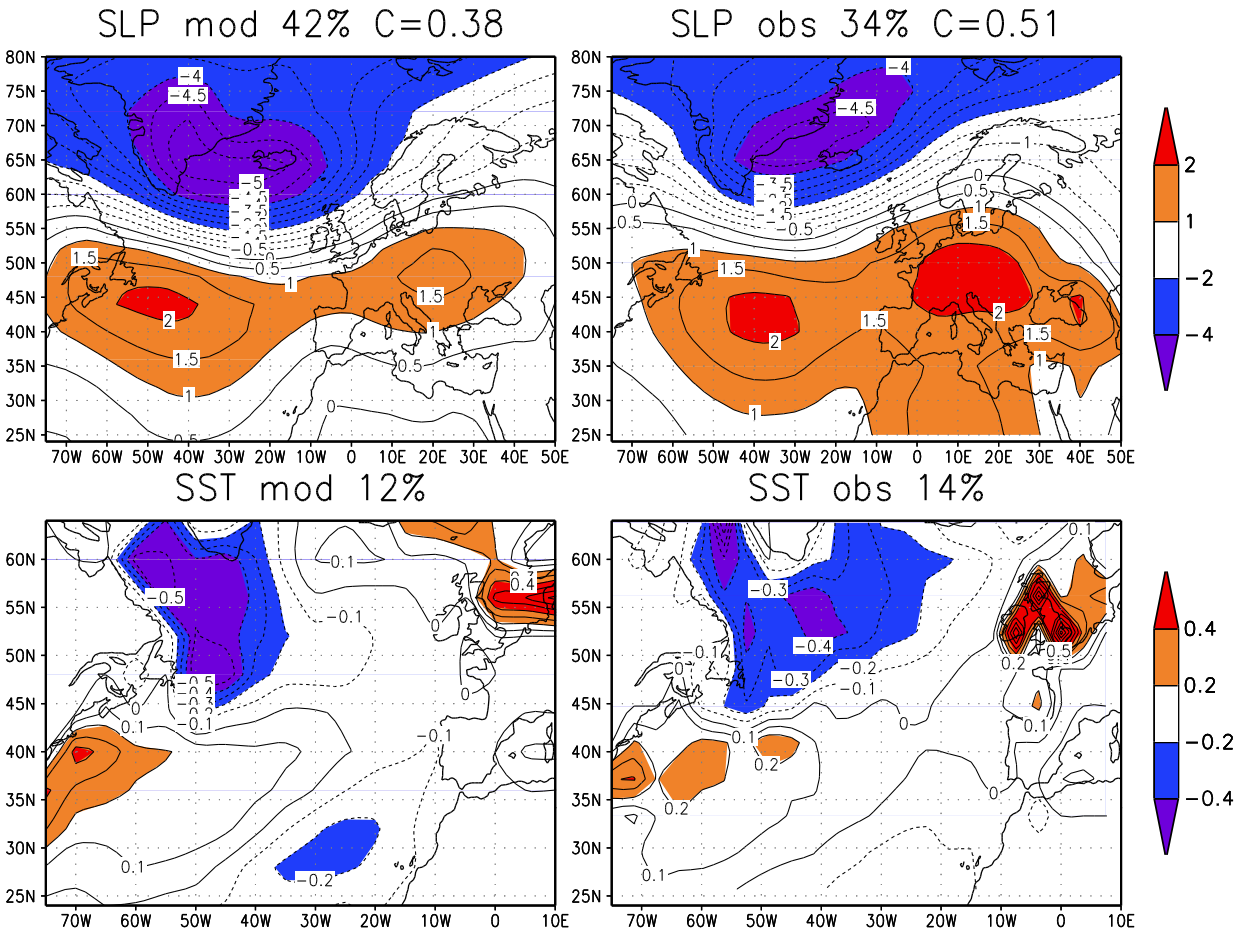


Fig. 1.11 The leading SVD modes of the sea level pressure (upper) and SST (lower) in the Northern Atlantic obtained from the model data (left) and observations (right).

Simulation of El Nino by the model agrees well with observations and it is described on the website in separate paper.

2. Comparison of models according to the IPCC Fourth Assessment Report

The comparison of simulations of some climatic characteristics by the model INM RAS and the other models, which took part in the international comparison 2005, is shown in the figure below. The full results of the comparison are presented in the chapter 8 of the IPCC Fourth Assessment Report.

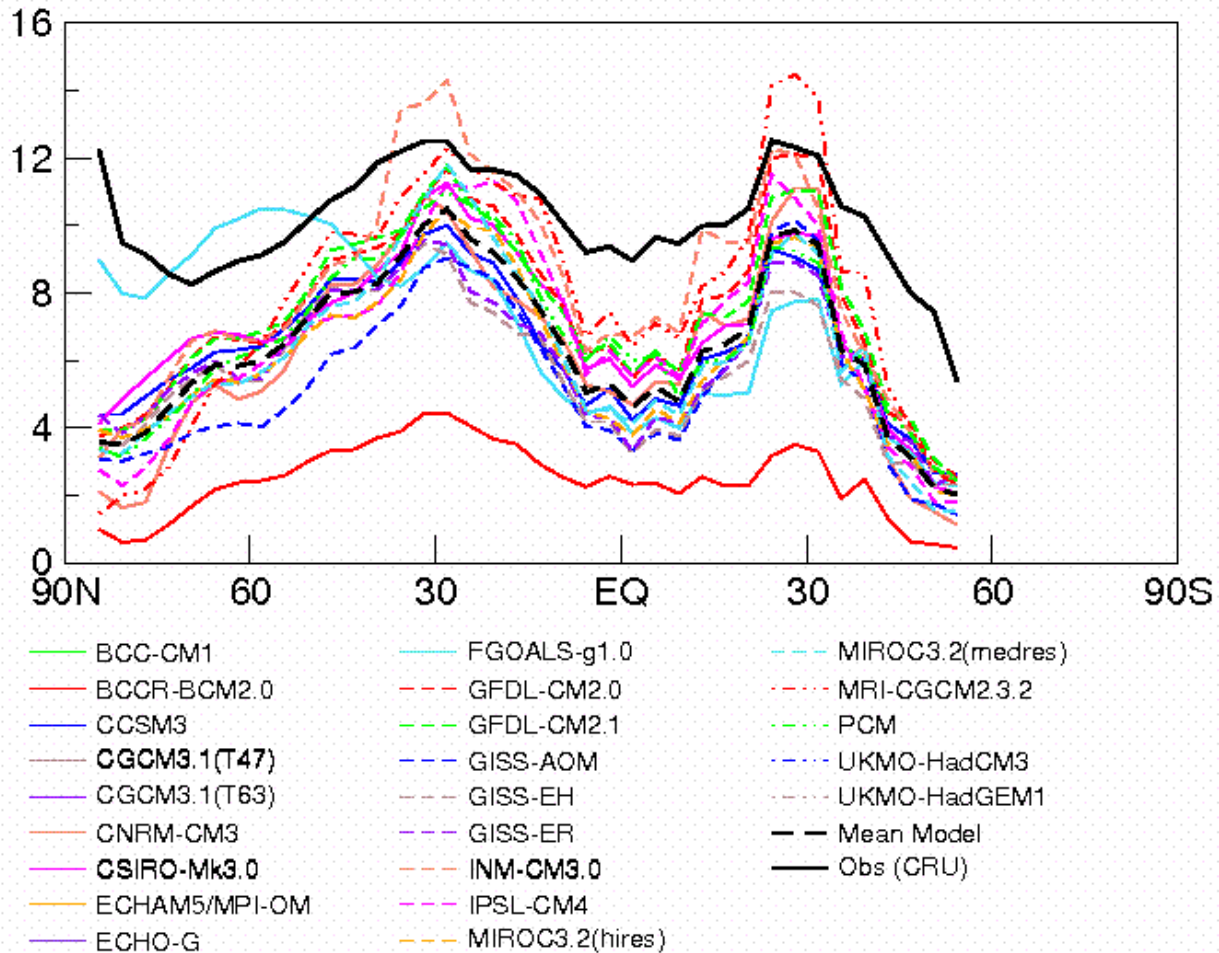


Fig. 2.1. The mean annual amplitude of the diurnal cycle of land surface temperature (degrees) obtained from the model data and observations (New et al, 1999).

The model amplitude of the diurnal cycle of land surface temperature is usually less than obtained from observations. It seems to be caused by a small number of levels in the soil which are used for solving the heat conduction equation. INM-CM3.0 has 23 levels and the depth of the first level is 1 cm, the amplitude of the diurnal cycle is one of the biggest of all models, and in northern subtropics it is even slightly more than the observed one.

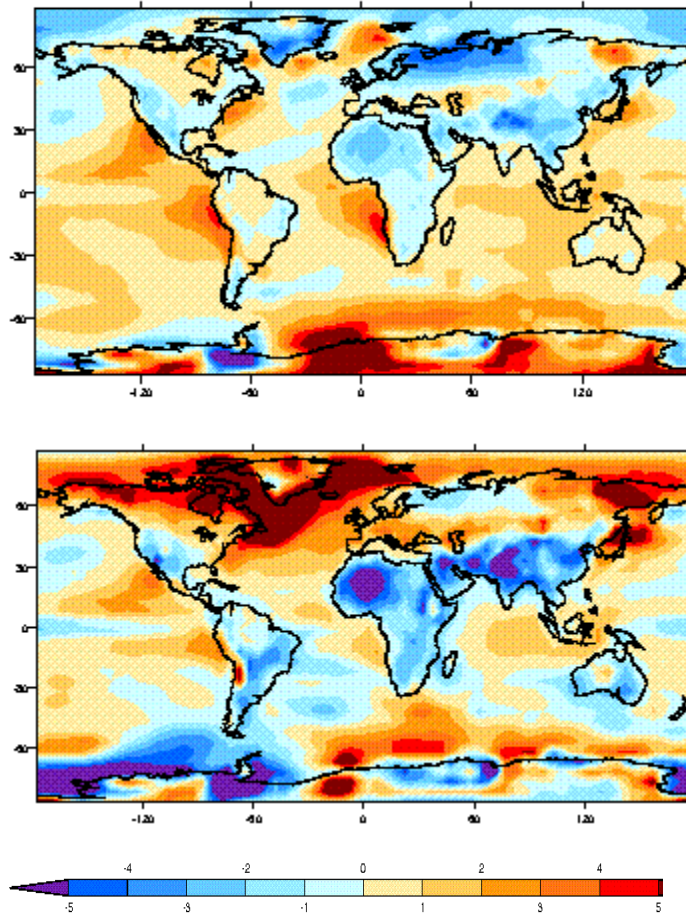


Fig 2.2. The mean annual error of 2m air temperature (degrees) obtained from the data of all models (upper) and INM RAS model (lower).

The highest errors are located in the north-western Atlantic, where the temperature is overestimated by 5 degrees. The error does not exceed 2 degrees in the tropics and subtropics with the exception of underestimation of temperature by 2-5 degrees in the Sahara and the south of Asia. However, INM-CM3.0 does not have significant errors connected with the underestimation of temperature in the north of Europe and Western Siberia which are typical for the most models

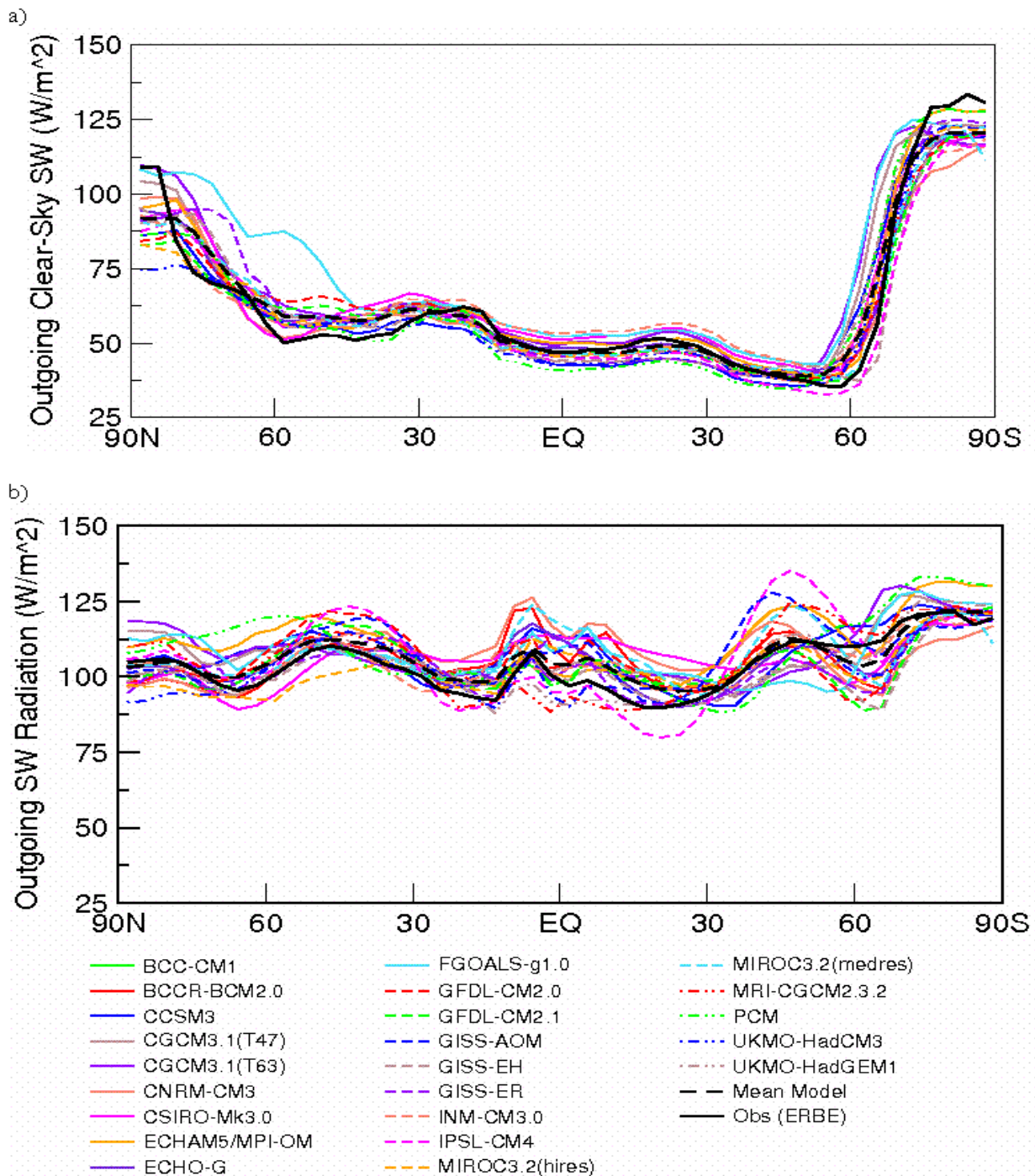


Fig. 2.3. Zonal mean annual outgoing shortwave radiation (W/m^2) for the clear sky (upper) and for the cloudy sky (lower) obtained from the model data and observations ERBE 1985-1988 (Barkstrom et al. 1989).

The clear sky outgoing solar radiation in the tropics and subtropics in INM model is one of the most intensive among all other models. It can be related with the overestimation of the surface albedo or the albedo of aerosols. However considering the cloudy sky case we can see that the difference between data of the model INM RAS and observations is not larger than for the other models.

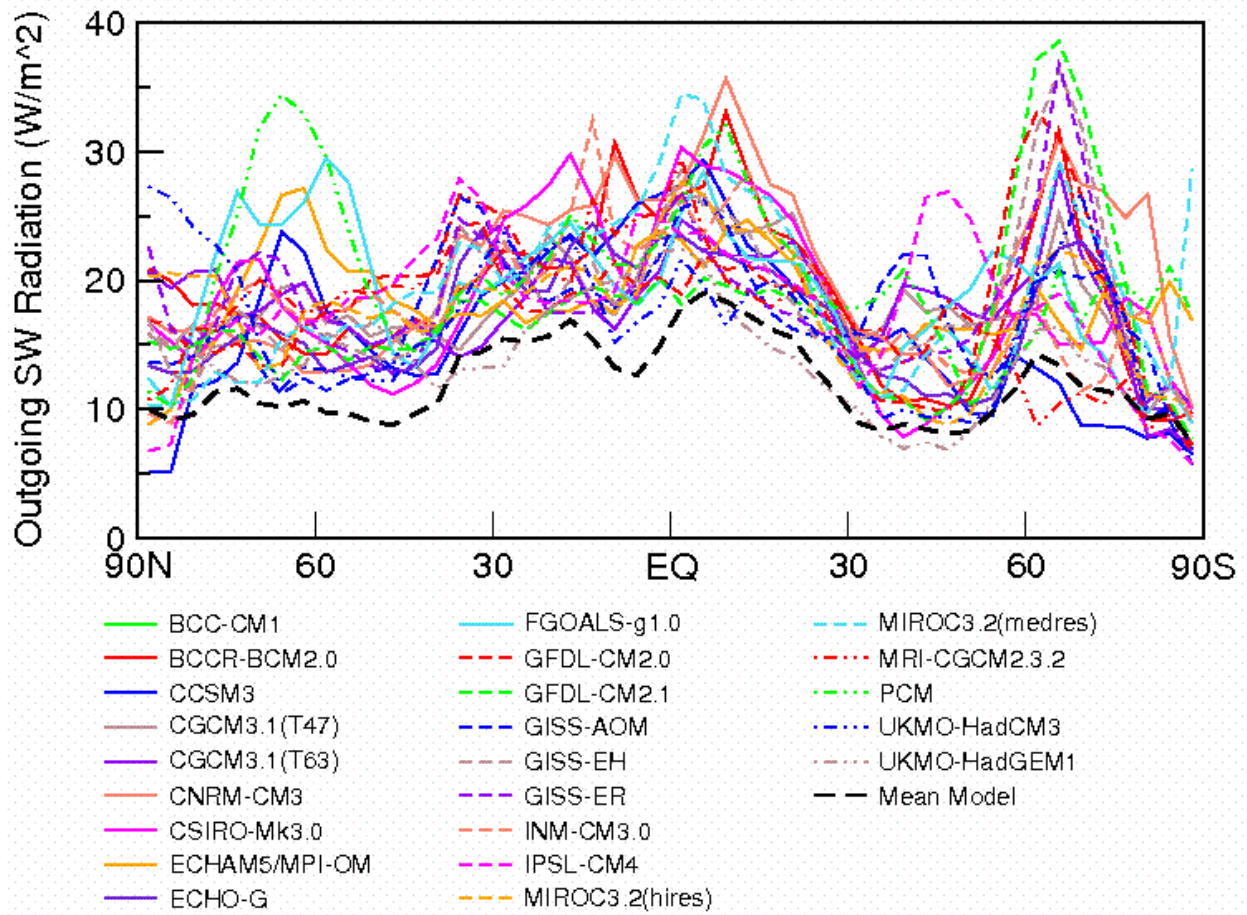


Fig. 2.4. Standard deviation of the TOA outgoing shortwave radiation (W/m^2) from the ERBE data 1985-1988 (Barkstrom et al. 1989) for all the models.

The error of geographical distribution of the outgoing shortwave radiation for the model of INM RAS does not go outside the interval of errors for all other models.

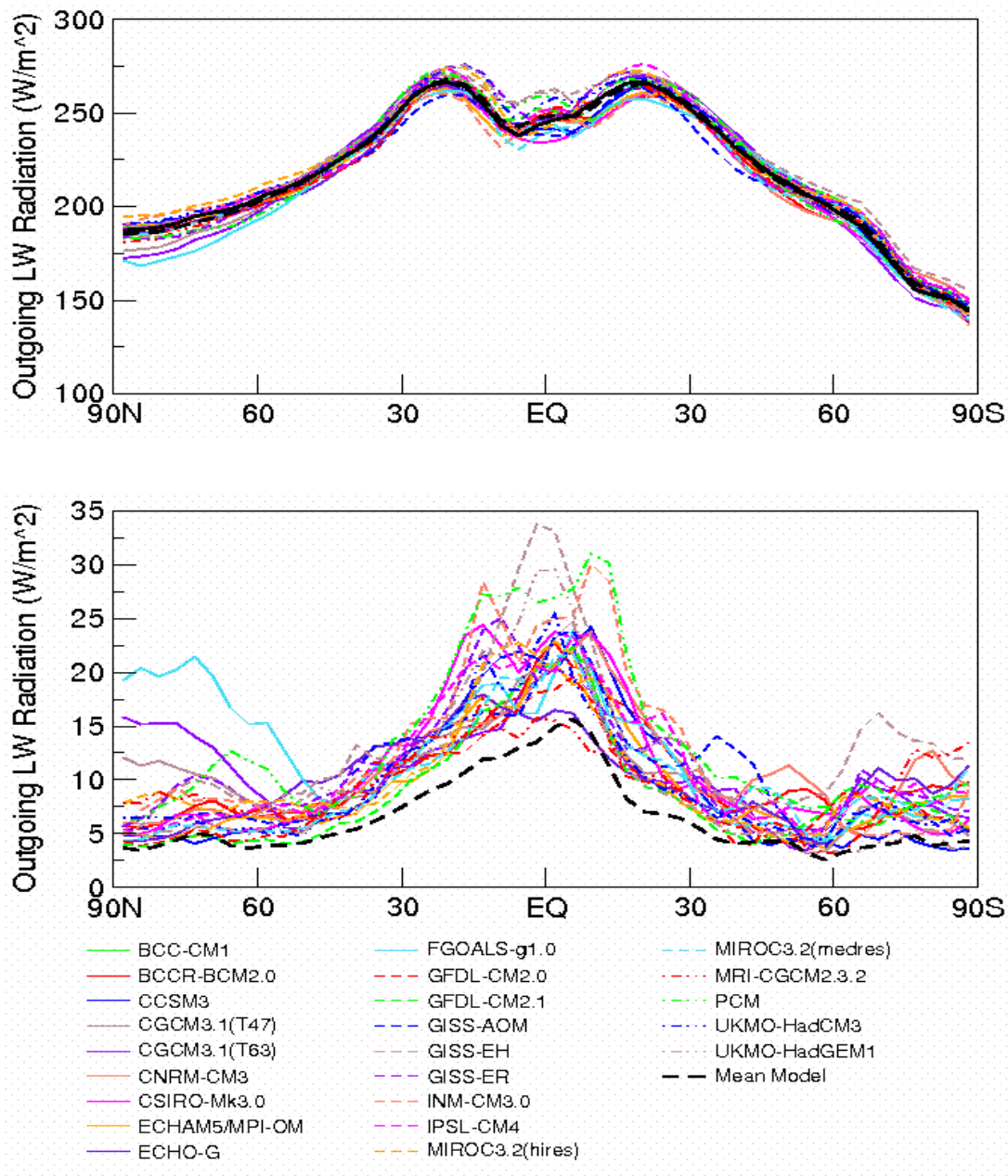


Fig. 2.5. Zonal mean annual outgoing long-wave radiation (W/m^2) (upper) and standard deviation of the model data from ERBE (lower).

The largest errors of the INM RAS model are located in the tropics astride the Equator. It is connected with the overestimation of precipitation in the Pacific Ocean astride the Equator because of the underestimation of SST on the Equator. The source of this model deficiency probably the coarse resolution of the ocean model, because it leads to the overestimation of upwelling near the Equator.

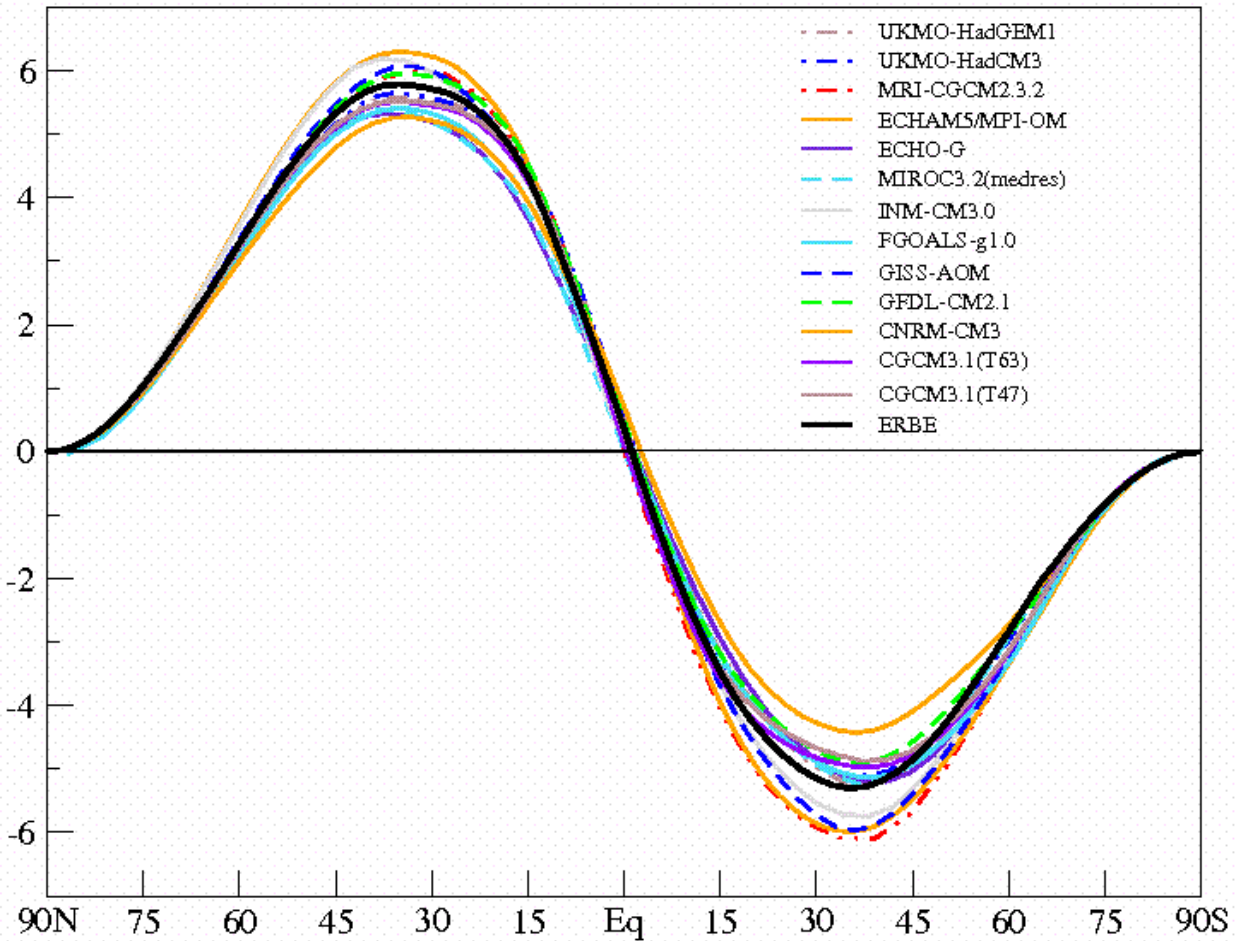


Fig.2.6. Heat flux in the atmosphere and in the ocean (PW) calculated using the TOA radiation balance from the model data and ERBE.

The heat flux in the atmosphere-ocean system of the INM RAS model is generally close to the observed and does not go outside the intermodel variability.

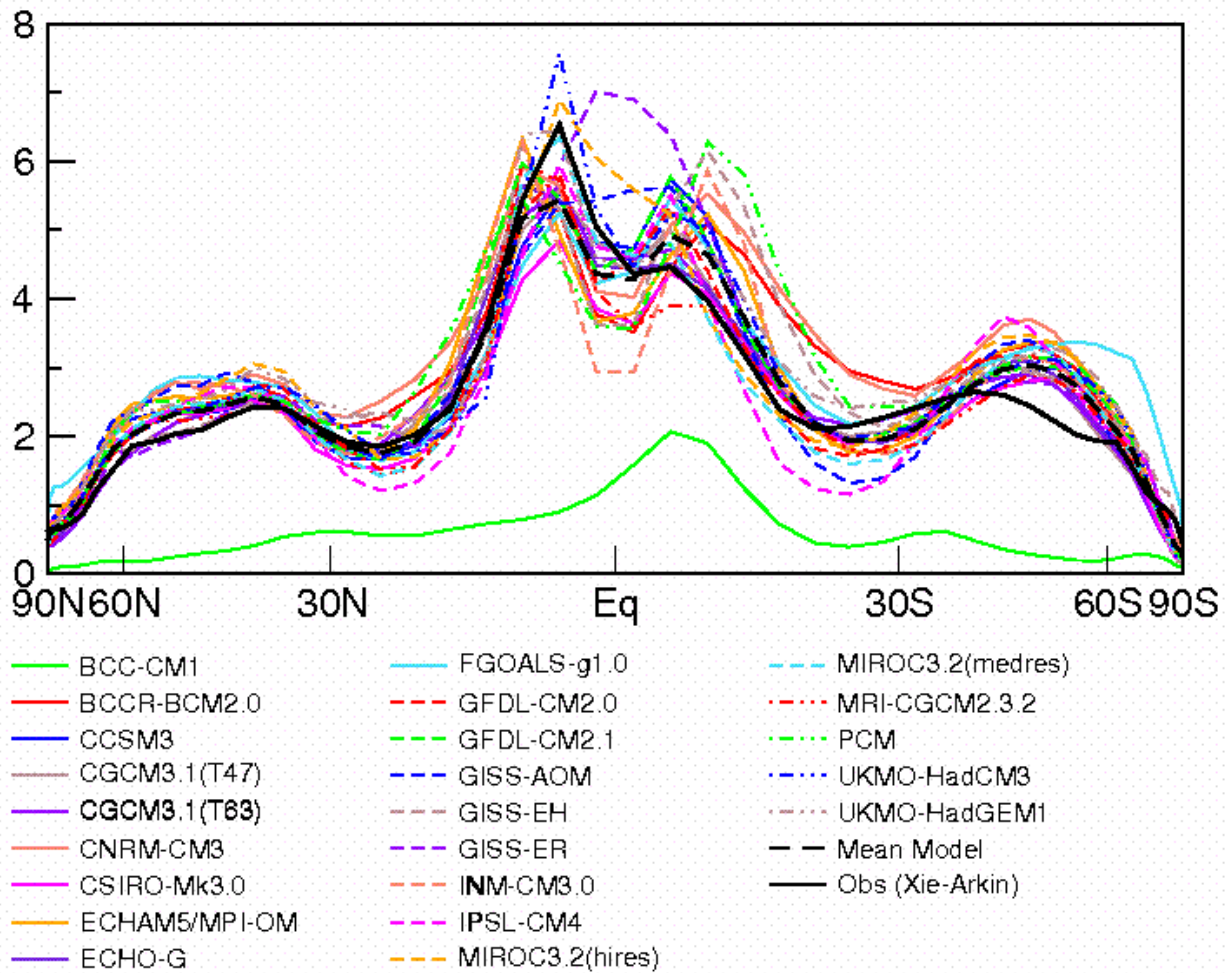


Fig. 2.7. Zonal mean annual precipitation (mm/s) obtained from the models data and observations (Xie, Arkin 1997).

INM-CM3.0 underestimates precipitation near the Equator and overestimates it to the south from the Equator. This generally occurs over the Pacific Ocean. Most of the other models have the same deficiency. At other latitudes the model data are close to observations.

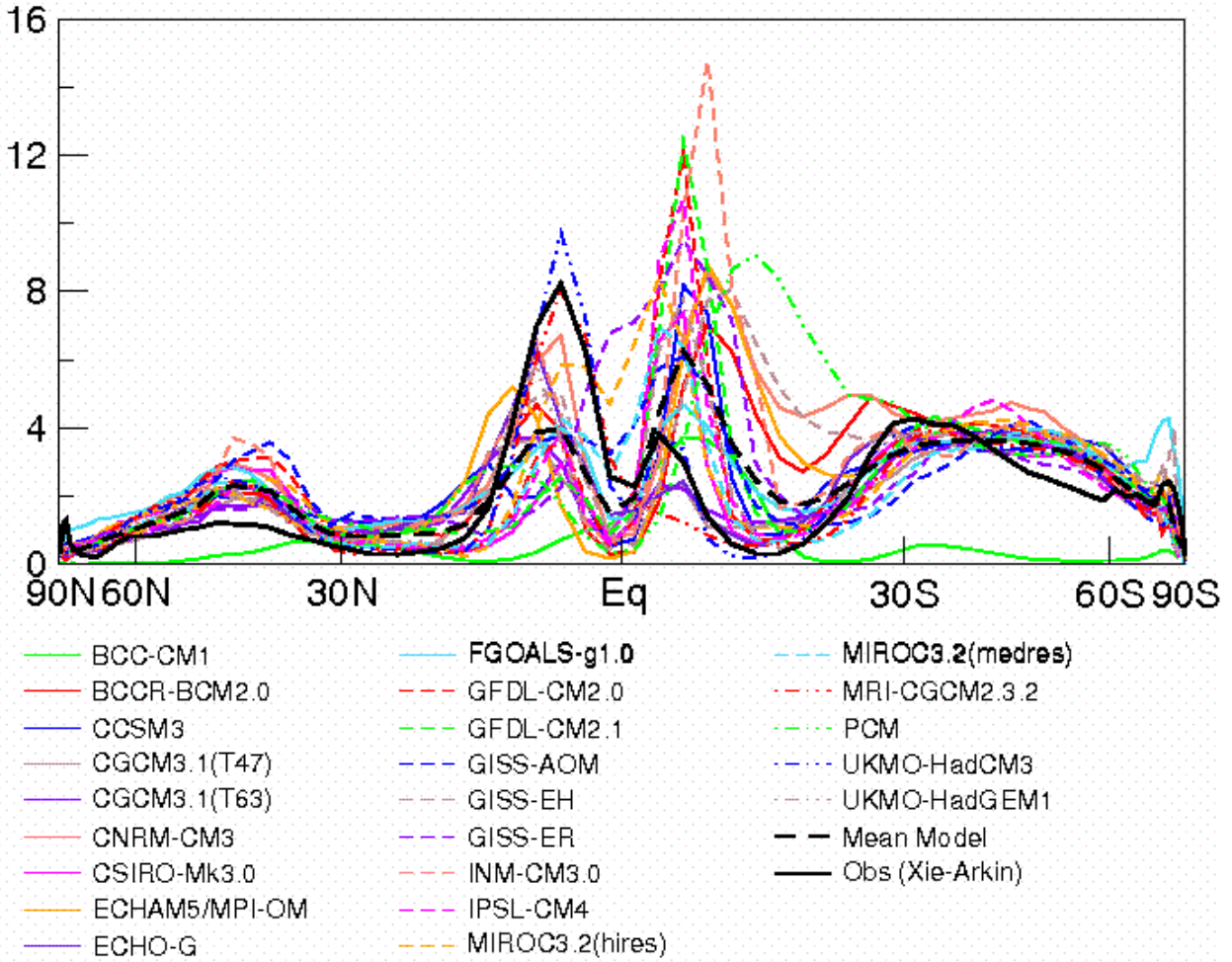


Fig. 2.8. Mean annual precipitation (mm/day) in the east part of the Pacific Ocean (120W-100W) obtained from the model data and observations (Xie, Arkin 1997).

Overestimation of precipitations to the south of the Equator by INM-CM3.0 and most of the other models is clearly observed in this figure. This error can be significantly reduced by increasing the resolution of the ocean model in latitude.

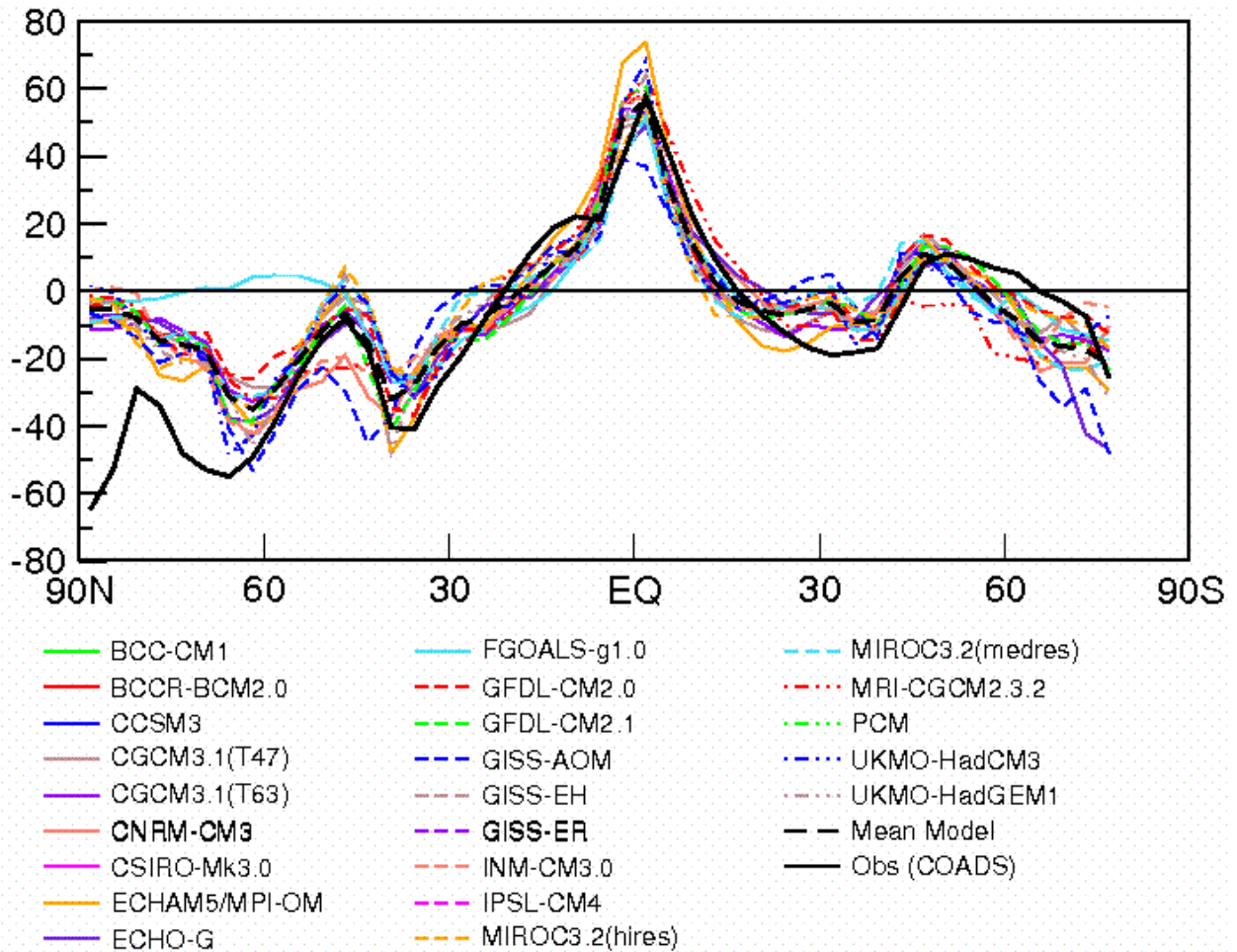


Fig. 2.9. Zonal mean annual heat flux towards the ocean (W/m^2) obtained from the model data and observations COADS (da Silva 1994).

Data of INM-CM3.0 do not go outside the intermodel variability and mainly agree with the estimate obtained from observations, with the exception of Arctic.

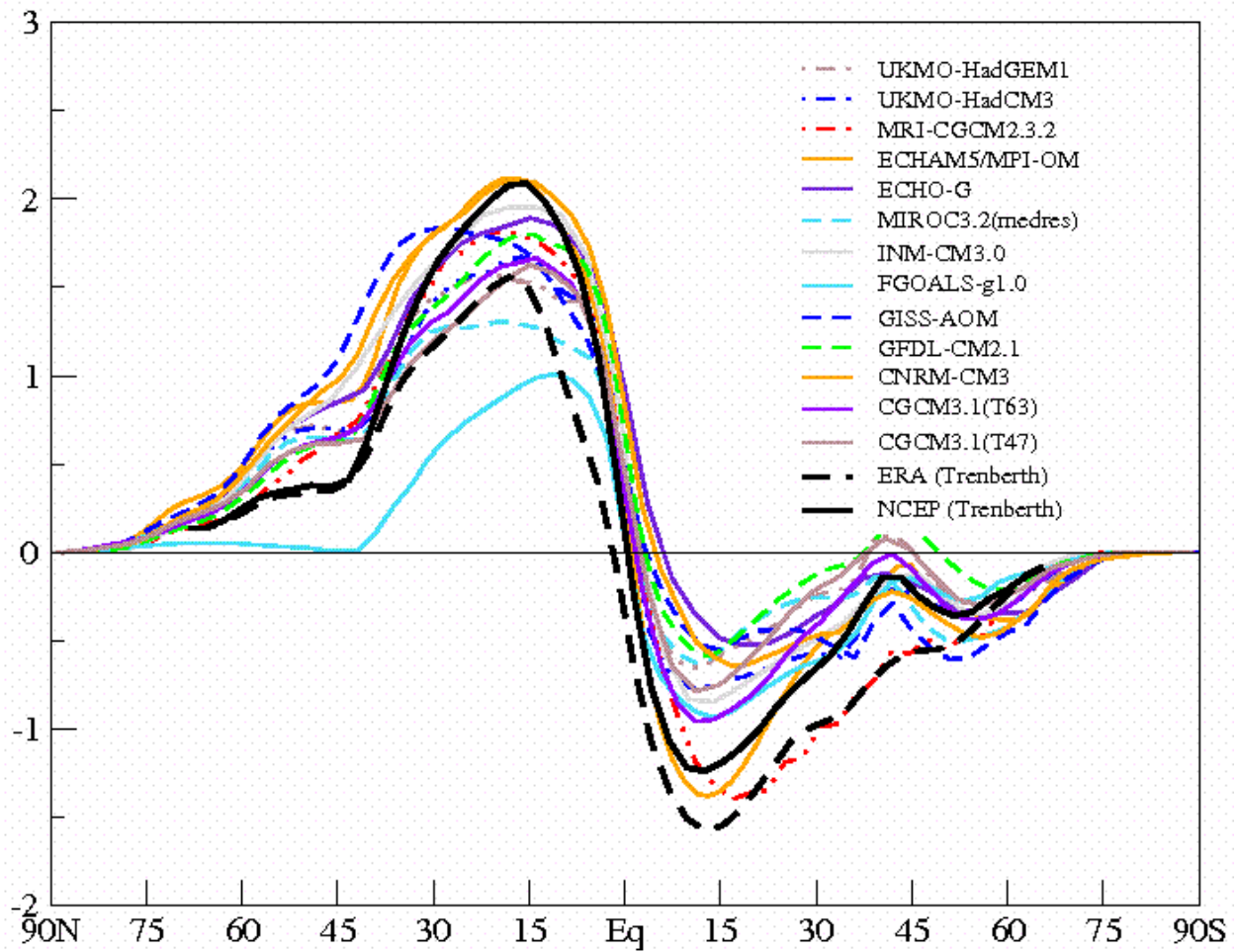


Fig. 2.10. Meridional heat flux in the ocean (PW) obtained from the models data and the its estimate from data of reanalysis NCEP and ERA.

Meridional heat flux by ocean in INM-CM3.0 is mainly agree to the estimate obtained from observations and does not exceed the intermodel variations.

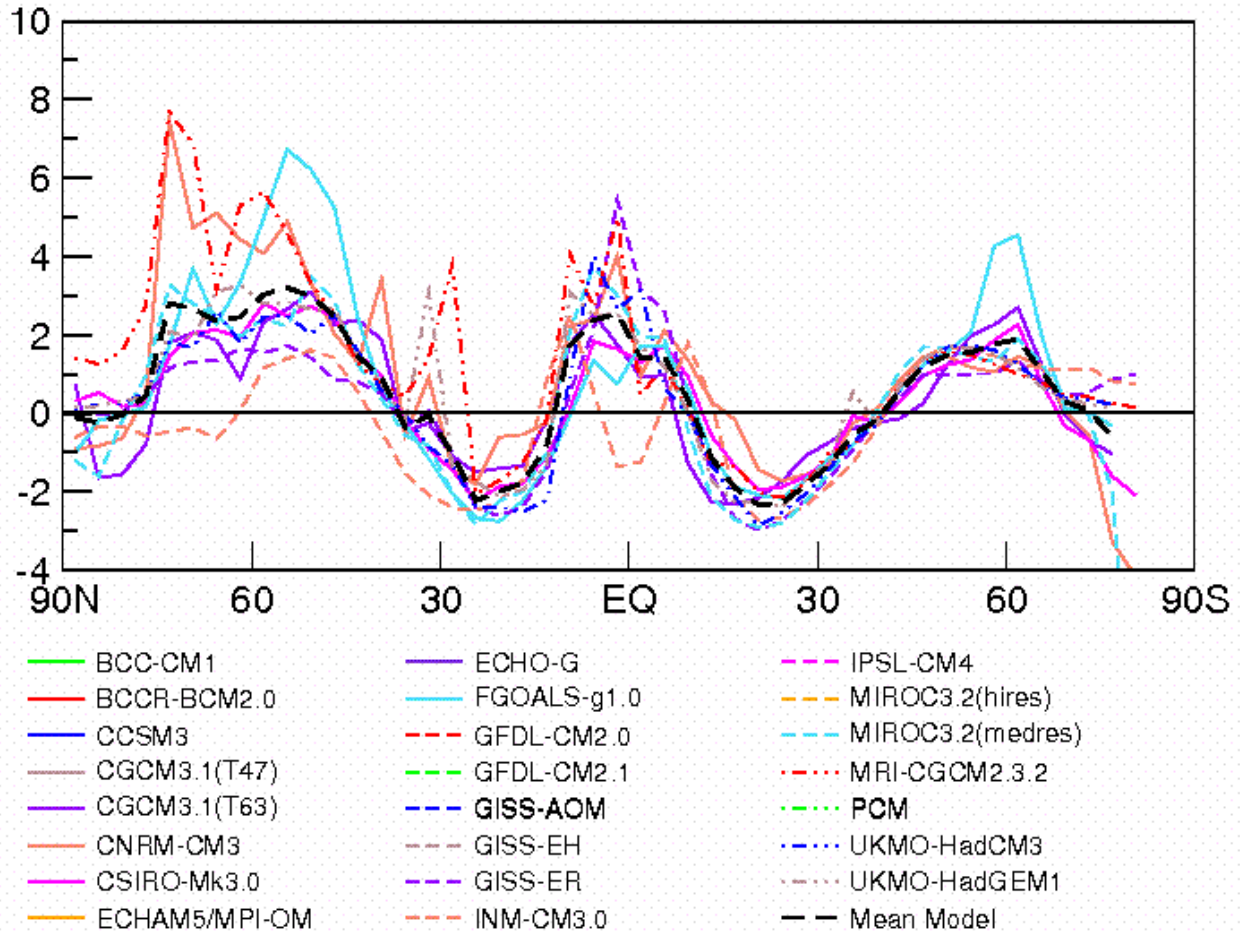


Fig. 2.11. Fresh water flux towards the ocean (mm/day) obtained from the models data.

Fresh water flux towards the ocean is less for INM-CM3.0 than for the other models. In Arctic it can be explained by introducing the correction of the fresh water, near the Equator - by underestimation of precipitation and in the middle latitudes the reason is not clear. It is possible that the total underestimation of the fresh water in INM-CM3.0 is because of there is no rivers inflow, which is considered separately, whereas for the other models it is added to the considered flow.

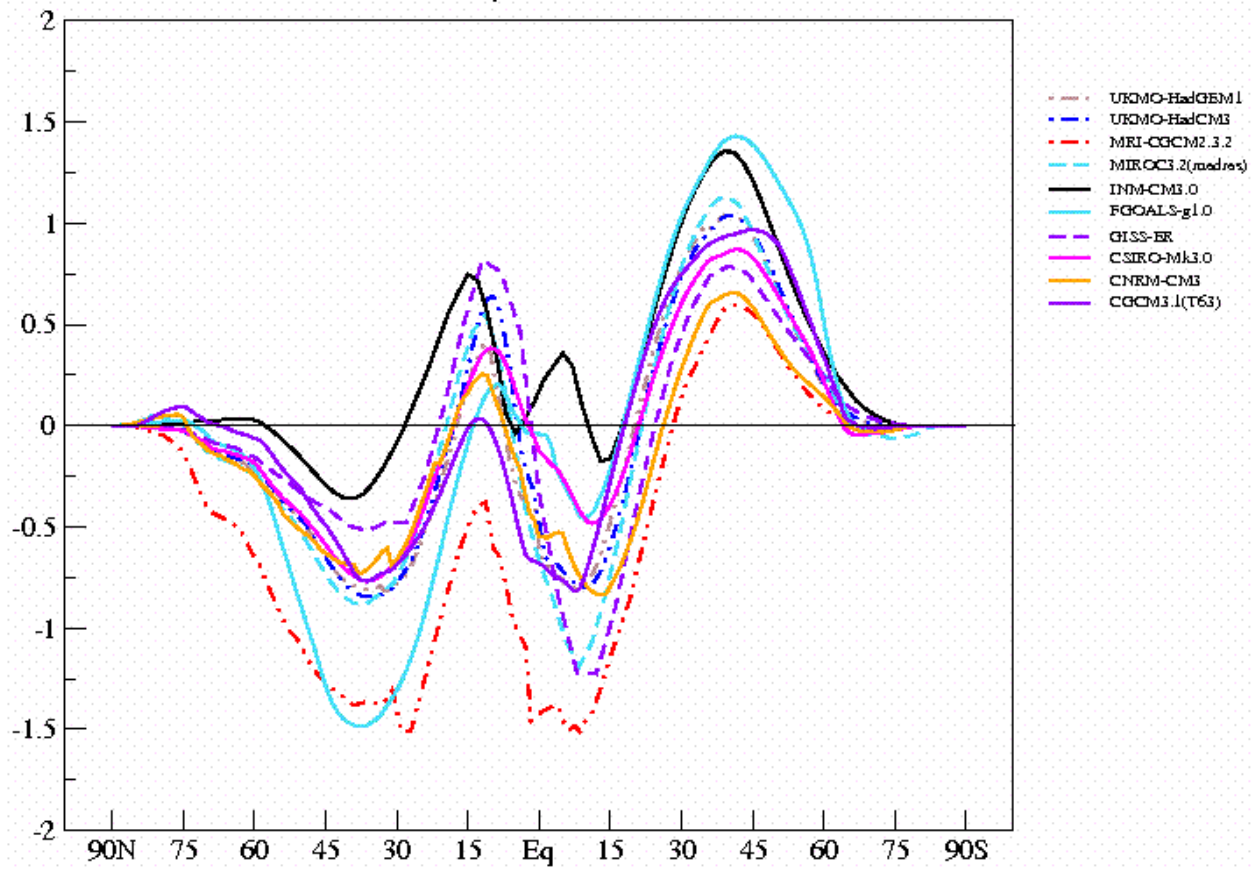


Fig. 2.12. Fresh water transport in the ocean (10^9 kg/s) obtained from model data.

Fresh water transport in the Northern Hemisphere is smallest in INM-CM3.0 because of the underestimation of the fresh water flux at the top of the ocean (see the previous figure).

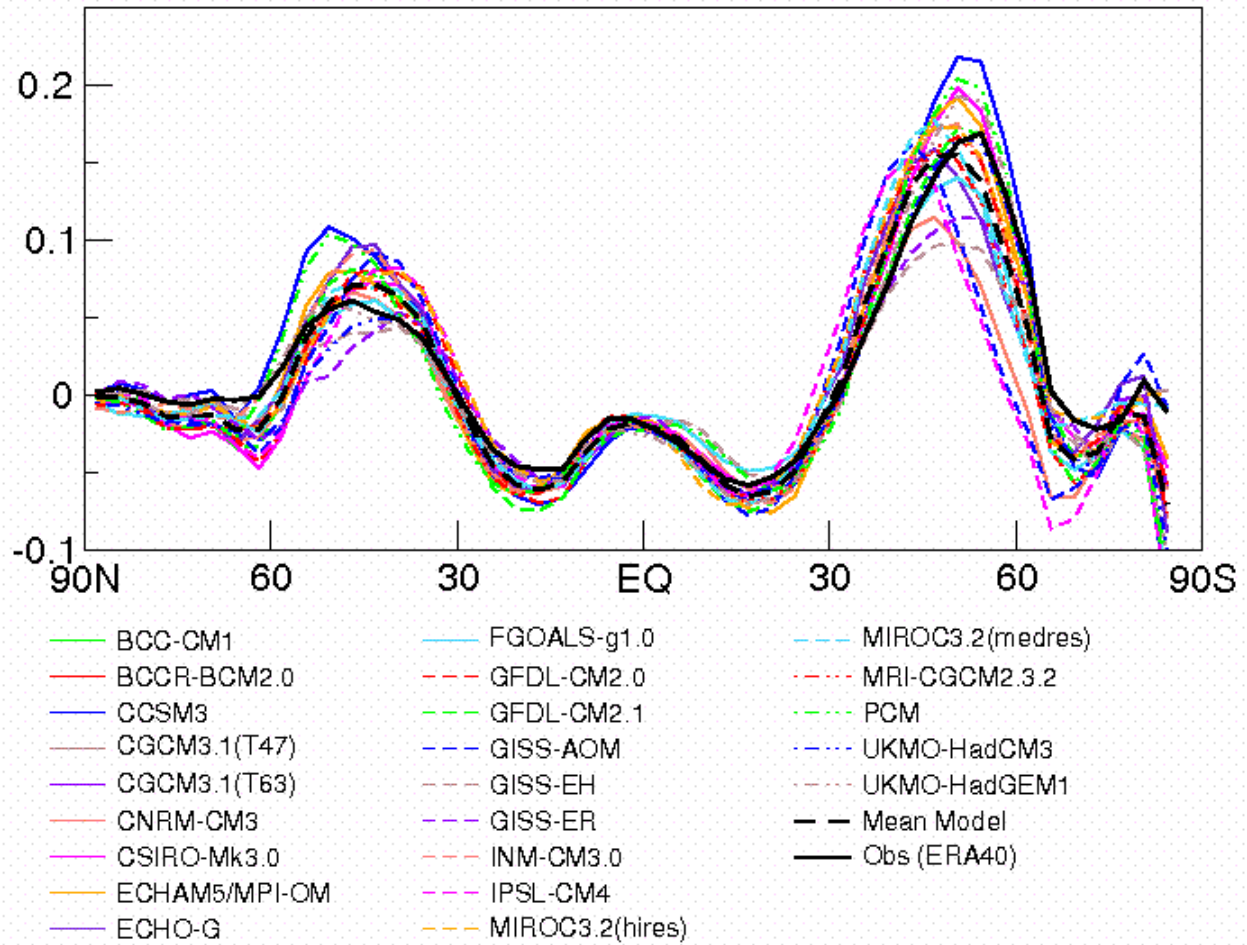


Fig. 2.13. Surface zonal wind stress (N/m^2) obtained from the model data and reanalysis ERA40.

Surface zonal wind stress of INM-CM3.0 agrees well with estimates by observations and does not go outside the intermodel variations.

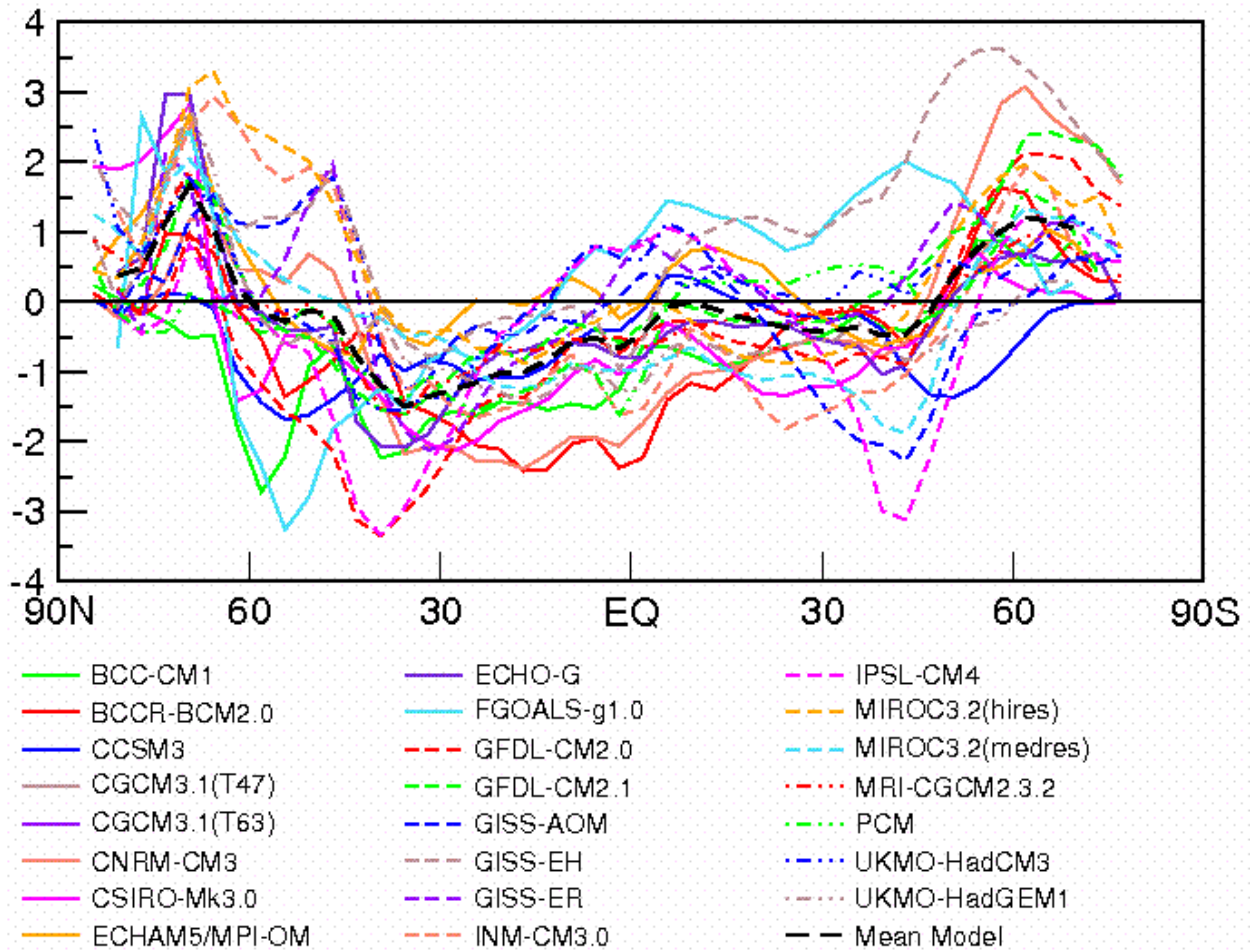


Fig. 2.14. Zonal error of SST simulation in the models (degrees).

SST simulation error of INM-CM3.0 is largest at the middle latitudes of the Northern Hemisphere and amounts here almost 3 degrees (mainly due to the Northern Atlantic). However even with this error the model does not go outside intermodel variations. INM-CM3.0 (like other models) has a tendency of the overestimation of temperature at the middle and high latitudes and underestimation in tropics and subtropics.

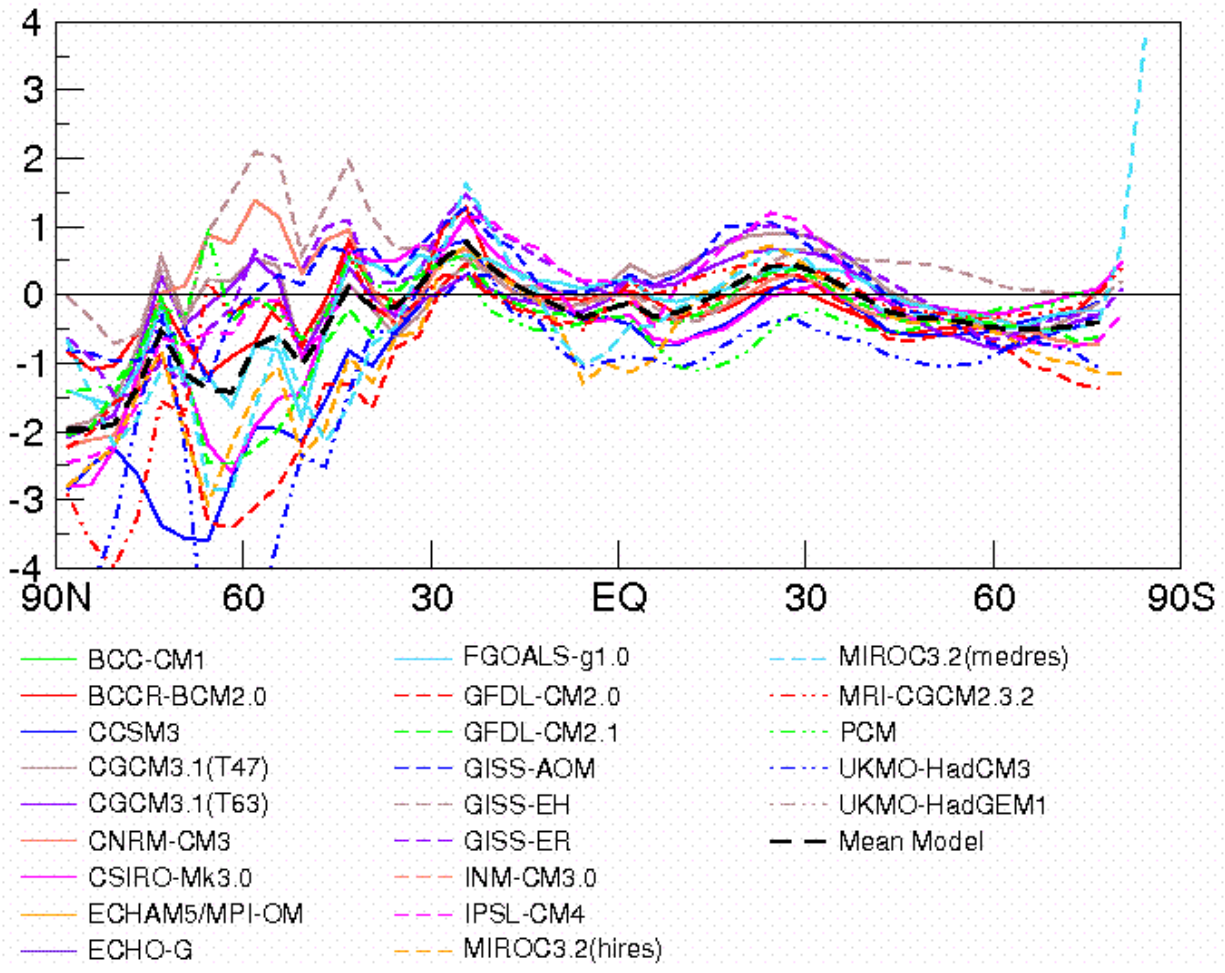


Fig. 2.15. Zonal mean annual error of simulation of the surface salinity (ppm) with respect to Levitus et al. (2005) obtained from model data.

Data of INM-CM3.0 are not shown on this figure.

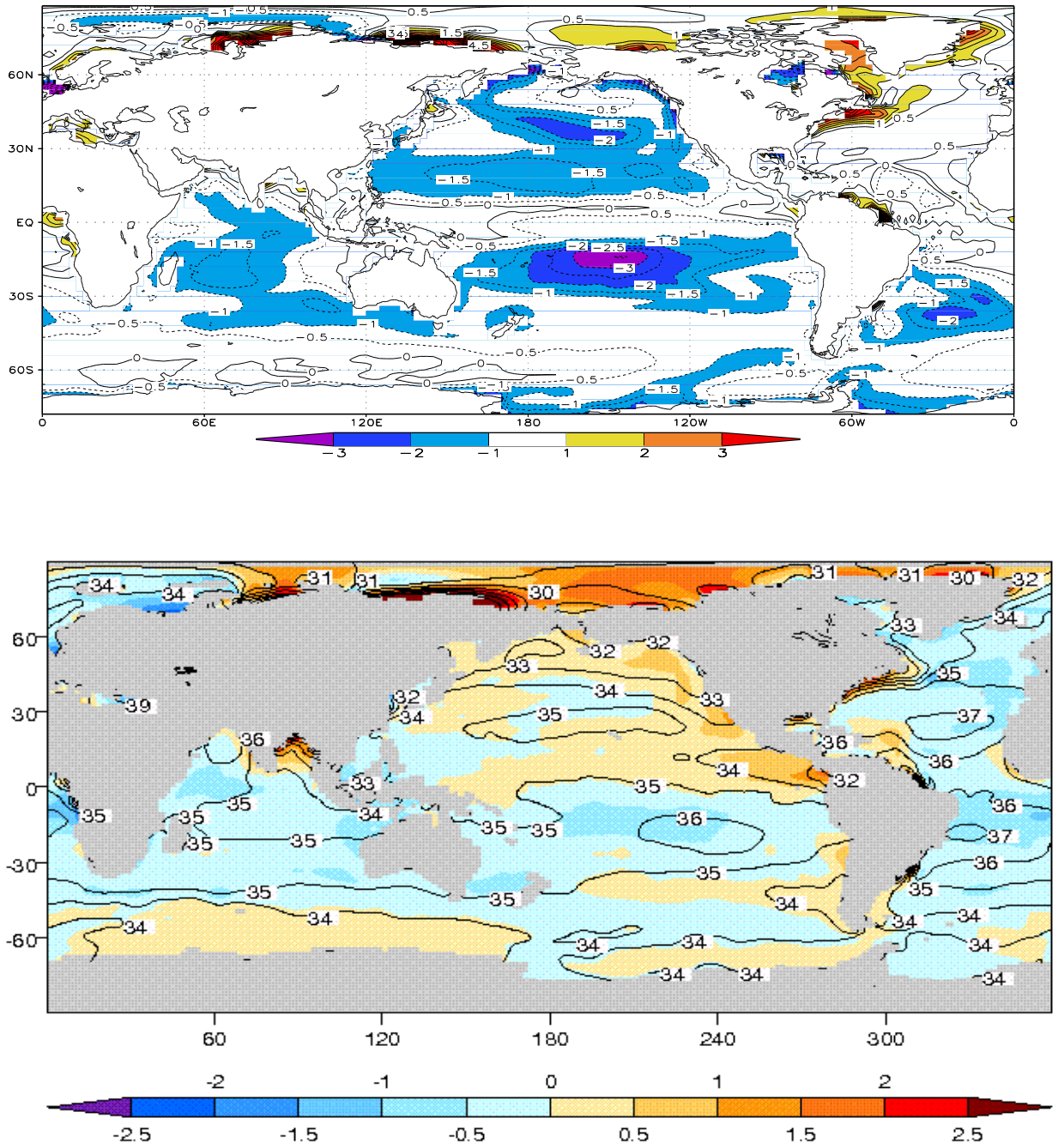


Fig.2.16. The mean annual error of simulation of the surface salinity (ppm) for INM-CM3.0 (upper) and for all models (lower)

It is evident that INM-CM3.0 has a strong underestimation of the salinity in the tropics and subtropics of the Indian and Pacific oceans. We suppose that the reason for it is in some errors of the ocean dynamics, and also some overestimation of precipitation. Simulation of salinity becomes better in the middle and high latitudes with the exception of the Northern Atlantic where the salinity is overestimated due to the excessive correction of the fresh water flux.

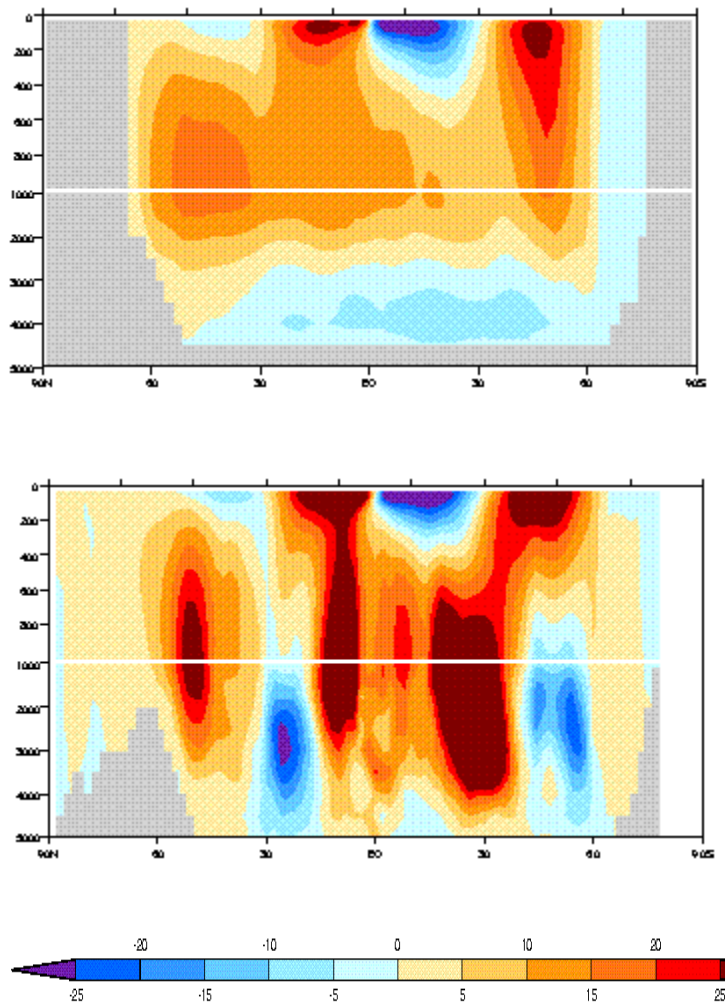


Fig. 2.17. Meridional stream function in the ocean (Sv) obtained from all model data (upper) and data of INM-CM3.0 (lower).

Detailed structure of the meridional circulation in the upper 500-meter layer of the ocean, is clearly seen on the figure both for all model average and for INM-CM3.0. But the circulation cells are considerably larger in INM-CM3.0 than in the all model average. It is probably caused by using of sigma-coordinates in the ocean model. However the comparison with the individual data from other models shows that many of them have similar deep waters circulation cells, which differ from model to model(not shown).

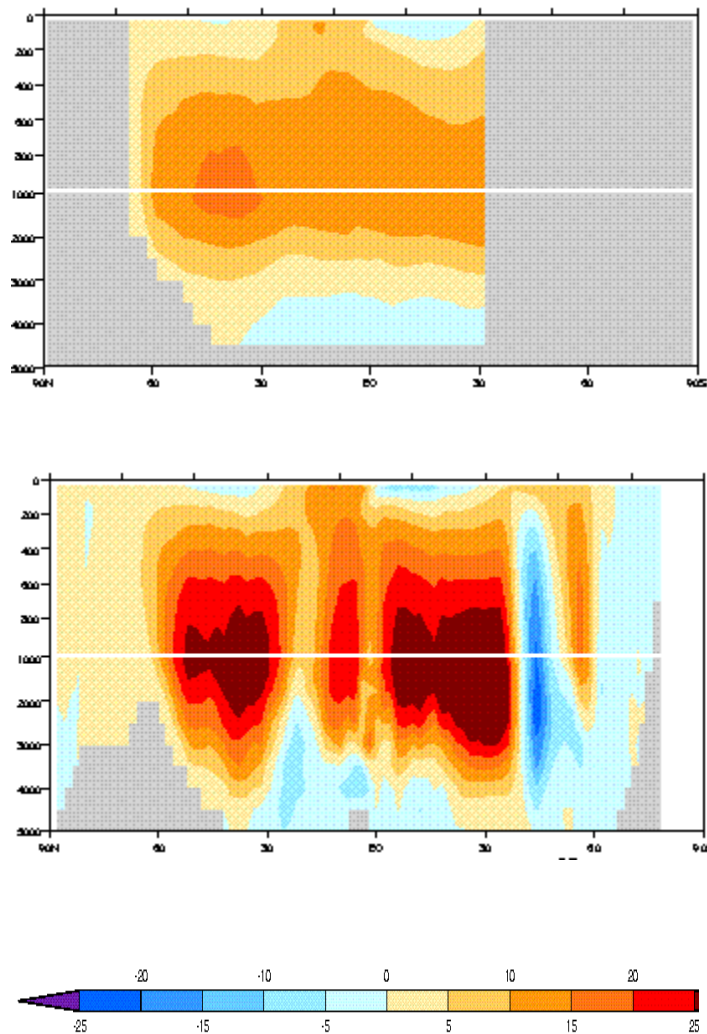


Fig. 2.18. Meridional stream function in the Atlantic (Sv) obtained from data of all models (upper) and INM-CM3.0 (lower).

According to all models data there is a flux from the south to the north in the upper layer of the ocean and below 1000 m it is inverse flux. This particularity exists also in INM-CM3.0. The mass flux in INM-CM3.0 is approximately in 1.5-2 times more, than the average flux calculated for all models.

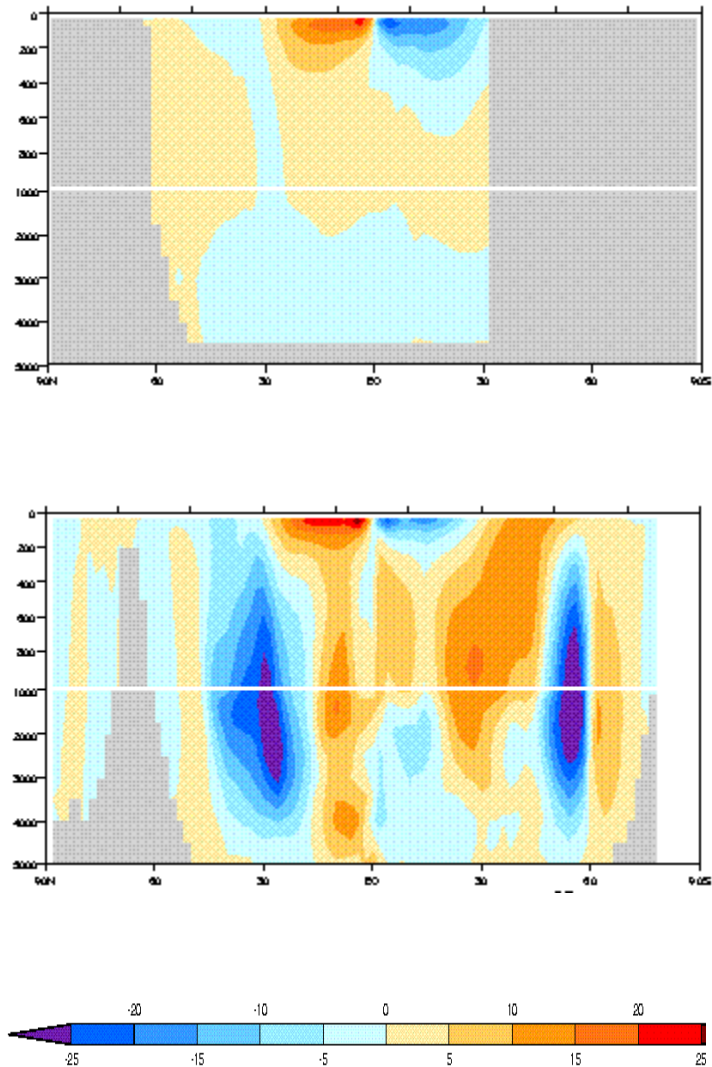


Fig. 2.19. Meridional stream function in the Pacific Ocean (Sv) obtained from data of all models (upper) and INM-CM3.0 (lower).

Upwelling in the near-surface layer of the Pacific Ocean and downwelling in the subtropics are represented both in INM-CM3.0 and all other models. Deep-ocean circulations in the Pacific Ocean obtained from INM-CM3.0 data do not agree with the average obtained from all models. However considering the other models individually we can see that there are also existing cells of the same size, but their sign and location change from one model to other. Moreover combining data of all models we obtain almost zero circulation.

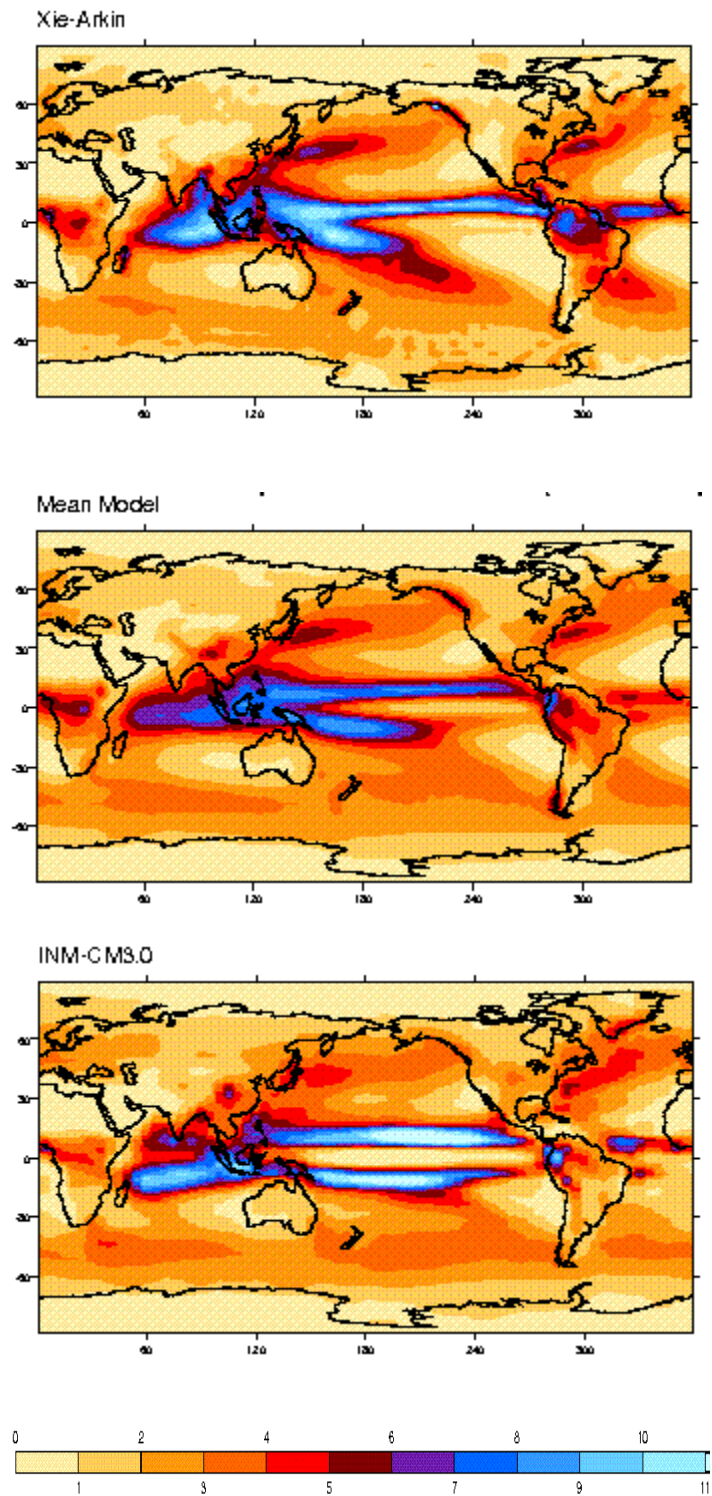


Fig. 2.20. Mean annual precipitation (mm/day) obtained from observations (upper) and data of INM-CM3.0 (lower).

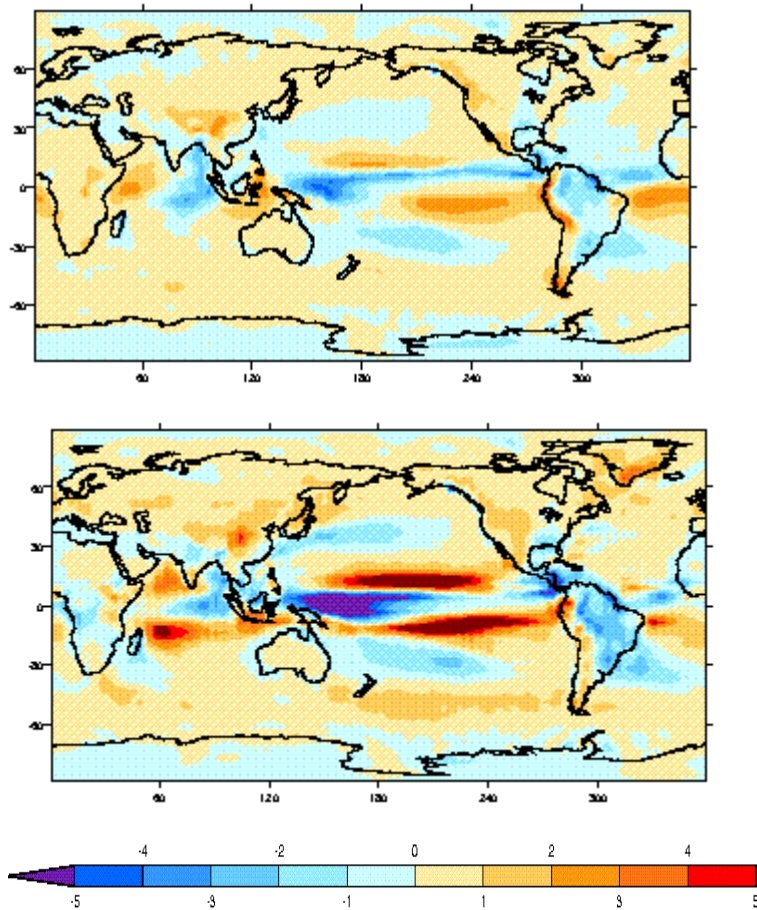


Fig. 2.21. Mean annual precipitation error (mm/day) calculated by average all model data (upper) and INM-CM3.0 (lower).

The main error of INM-CM3.0 simulation of precipitation is its underestimation near the Equator in the west part of the Pacific Ocean and its overestimation directly to the north and south from the Equator. Furthermore there is the underestimation of precipitations in the Central and the most part of South America. These errors are caused by the overestimated upwelling in the Equator and its spreading to the west of the Pacific Ocean. As a result, SST becomes in 2 degrees lower than the observed value. The above listed errors of simulation of the precipitation in the tropics are typical for all models and also for the average calculated by all models data. However it should be noted that precipitation is less for the averaged data than for INM-CM3.0.

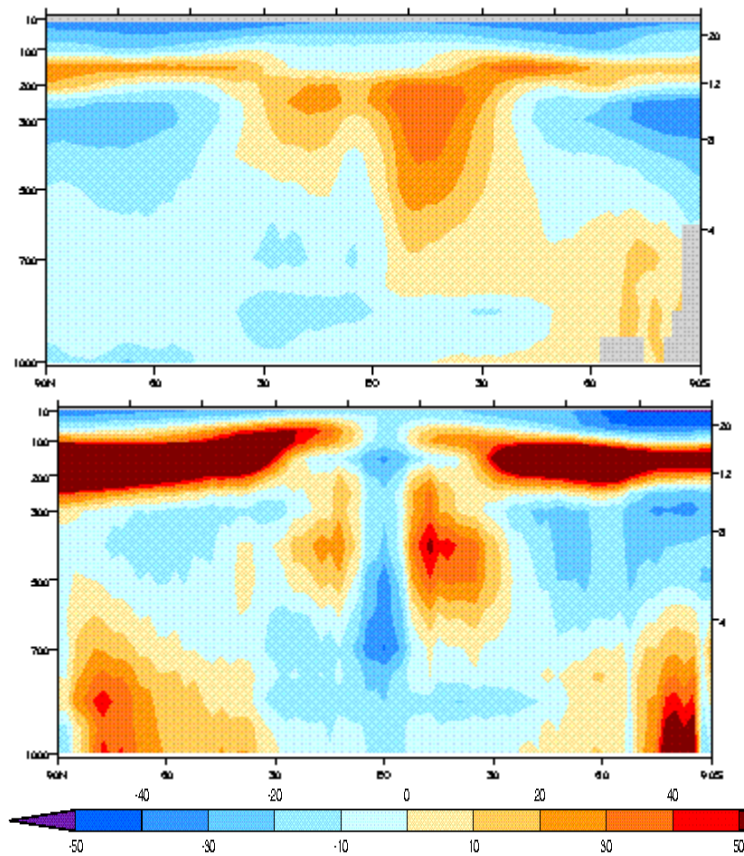


Fig. 2.22. Relative error of simulation of the specific humidity of air (%) obtained from all models data (upper) and INM-CM3.0 (lower).

The main error of specific humidity in INM-CM3.0 is located near the tropopause where the humidity is overestimated in spite of the lower temperature. Humidity is also overestimated in high latitudes of the both hemispheres. Humidity errors in the tropics refer to the errors of the precipitation distribution. As a whole the errors level in INM-CM3.0 corresponds to the error level of most other models (not shown).

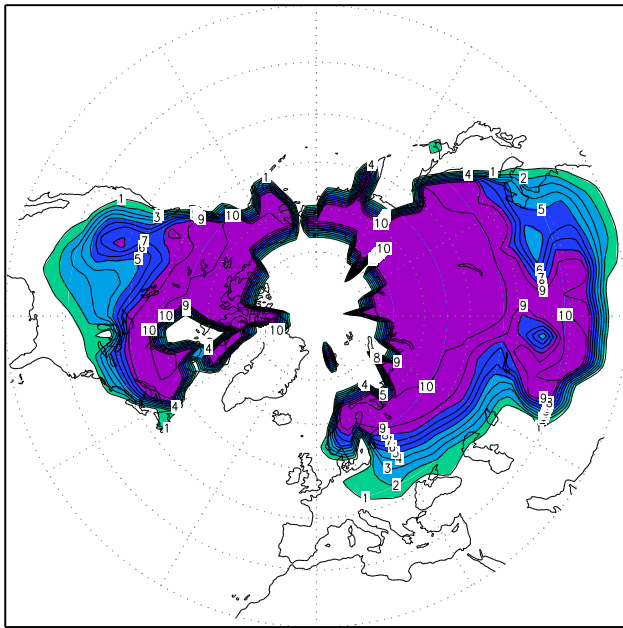
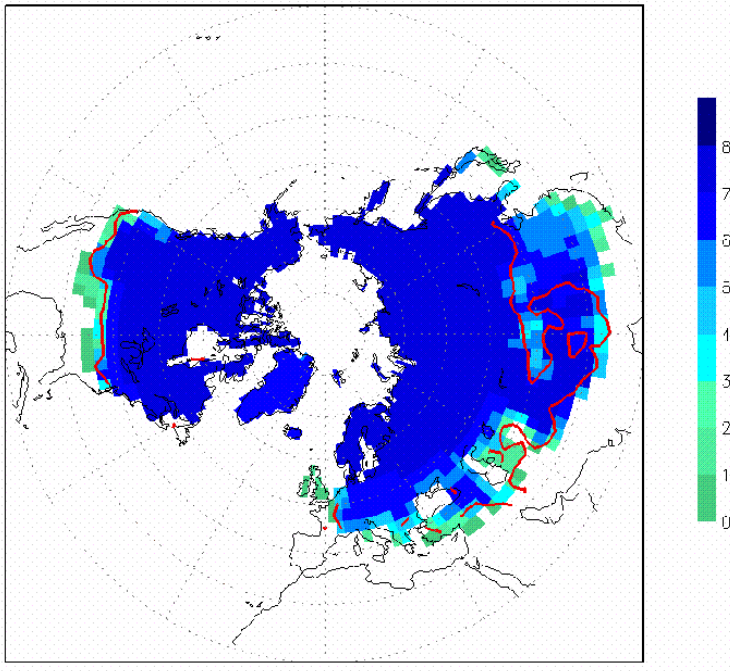


Fig. 2.23. Part of the surface covered by snow in February (the full coverage corresponds 10) obtained from data of all models and from observations (Robinson, Frei 2000) (upper) and from data of INM-CM3.0 (lower).

In general INM-CM3.0 represents correctly the boundary of the snow cover in February. Errors have the maximum values in the western and southern Europe, where the snow cover area is underestimated by the model because of the overestimation of temperature and probably because the snow freezeback after melting is not taken into account.

As the whole INM-CM3.0 represents well the observed climate. The errors mostly do not exceed the intermodel variations. The largest errors of INM-CM3.0 are connected with underestimation of SST near the Equator in the Pacific Ocean and also with overestimation of SST in the north-west of Atlantic. Probably this is caused by the excessive correction of the fresh water flux in the high latitudes. Furthermore there are the desalination and cooling of the upper layer of the ocean and also warming and salinity increasing of deep-sea layers.

References

- I. Barkstrom B., Harrison E., Smith G., Green R., Kibler J., Cess R. and ERBS science team. Earth Radiation Budget Experiment (ERBE) archival and April 1985 results. *Bull. Amer. Met. Soc.*, 1989, V.70, p.1254-1262.
- II. da Silva A.M., Young C.C., Levitus S. Atlas of surface marine data 1994. NOAA Atlas NESDES 6. Available from US Dept. Commerce, NODC, User Services Branch, NOAA/NESDIS E/OC21, Washington DC, 20233, USA.
- III. Levitus S., Antonov J., Boyer T. Warming of the world ocean, 1955-2003. *Geophys. Res. Lett.*, 2005, V.32, L02604, doi: 10.1029/20046LO21592.
- IV. New M., Hulne M., Jones P.D. Representing twentieth-century space – time climate variability. Part 1. Development of a 1961-90 mean monthly terrestrial climatology. *J. Climate*, 1999, V.12, p.829-856.
- V. Robinson D.A., Frei A. Seasonal variability of northern hemisphere snow extent using visible satellite data. *Professional Geographer*, 2000, V.51, p.307-314.
- VI. Xie P., Arkin P.A. Global precipitation: A 17-year monthly analysis based on gauge observations, satellite estimates, and numerical model outputs. *Bull. Amer. Met. Soc.*, 1997, V.78, p.2539-2558.